

# Shelf break exchange processes influence the availability of the northern shortfin squid, *Illex illecebrosus*, in the Northwest Atlantic

Sarah L. Salois<sup>1</sup>  | Kimberly J. W. Hyde<sup>1</sup>  | Adrienne Silver<sup>2</sup>  |  
 Brooke A. Lowman<sup>3</sup>  | Avijit Gangopadhyay<sup>4</sup>  | Glen Gawarkiewicz<sup>2</sup>  |  
 Anna J. M. Mercer<sup>1</sup>  | John P. Manderson<sup>5</sup> | Sarah K. Gaichas<sup>6</sup>  |  
 Daniel J. Hocking<sup>7</sup>  | Benjamin Galuardi<sup>4,7</sup> | Andrew W. Jones<sup>1</sup> | Jeff Kaelin<sup>8</sup> |  
 Greg DiDomenico<sup>8</sup> | Katie Almeida<sup>9</sup> | Bill Bright<sup>10</sup> | Meghan Lapp<sup>11,12</sup>

<sup>1</sup>NOAA Northeast Fisheries Science Center, 28 Tarzwell Drive, Narragansett, Rhode Island 02882, USA

<sup>2</sup>Department of Physical Oceanography, Woods Hole Oceanographic Institution, Woods Hole, Massachusetts 02543, USA

<sup>3</sup>Virginia Marine Resources Commission, 380 Fenwick Road, Fort Monroe, Virginia 23651, USA

<sup>4</sup>School for Marine Science and Technology, University of Massachusetts Dartmouth, 836 South Rodney French Blvd, New Bedford, Massachusetts 02744, USA

<sup>5</sup>OpenOcean Research, PO Box 594, Blue Hill, Maine 04614, USA

<sup>6</sup>NOAA Northeast Fisheries Science Center, 166 Water Street, Woods Hole, Massachusetts 02543, USA

<sup>7</sup>Greater Atlantic Regional Fisheries Office, NOAA National Marine Fisheries Service, 55 Great Republic Drive, Gloucester, MA 01930, USA

<sup>8</sup>Lund's Fisheries, Inc., 997 Ocean Drive, Cape May, New Jersey 08204, USA

<sup>9</sup>The Town Dock, 45 State Street, Narragansett, Rhode Island 02882, USA

<sup>10</sup>F/V Retriever, F/V Defiance, and Hooked Up Seafood, 615 Goshen Rd, Cape May Court House, New Jersey 08210, USA

<sup>11</sup>Seafreeze Ltd., 100 Davisville Pier, North Kingstown, Rhode Island 02852, USA

<sup>12</sup>Seafreeze Shoreside, 75 State Street, Narragansett, Rhode Island 02882, USA

## Correspondence

Sarah L. Salois, NOAA Northeast Fisheries Science Center, 28 Tarzwell Drive, Narragansett, RI 02882, USA.  
 Email: [ssalois@umassd.edu](mailto:ssalois@umassd.edu)

## Present address

Sarah L. Salois, School for Marine Science and Technology, University of Massachusetts Dartmouth, 836 South Rodney French Blvd, New Bedford, Massachusetts 02744, USA.

## Abstract

The United States Northern Shortfin squid fishery is known for its large fluctuations in catch at annual scales. In the last 5 years, this fishery has experienced increased availability of *Illex illecebrosus* along the Northeast US continental shelf (NES), resulting in high catch per unit effort (CPUE) and early fishery closures due to quota exceedance. The fishery occurs within the Northwest Atlantic, whose complex dynamics are set up by the interplay between the large-scale Gulf Stream, mesoscale eddies, Shelfbreak Jet, and shelf-slope exchange processes. Our ability to understand and quantify this regional variability is requisite for understanding the availability patterns of *Illex*, which are largely influenced by oceanographic conditions. In an effort to advance our current understanding of the seasonal and interannual variability in this species' relative abundance on the NES, we used generalized additive models to examine the relationships between the physical environment and hotspots of productivity to changes in CPUE of

This is an open access article under the terms of the [Creative Commons Attribution-NonCommercial-NoDerivs](https://creativecommons.org/licenses/by-nc-nd/4.0/) License, which permits use and distribution in any medium, provided the original work is properly cited, the use is non-commercial and no modifications or adaptations are made.

© 2023 The Authors. *Fisheries Oceanography* published by John Wiley & Sons Ltd. This article has been contributed to by U.S. Government employees and their work is in the public domain in the USA.

*I. illecebrosus* in the Southern stock component, which comprises the US fishery. Specifically, we derived oceanographic indicators by pairing high-resolution remote sensing data and global ocean reanalysis physical data to high-resolution fishery catch data. We identified a suite of environmental covariates that were strongly related to instances of higher catch rates. In particular, bottom temperature, warm core rings, subsurface features, and frontal dynamics together serve as indicators of habitat condition and primary productivity hotspots, providing great utility for understanding the distribution of *Illex* with the potential for forecasting seasonal and interannual availability.

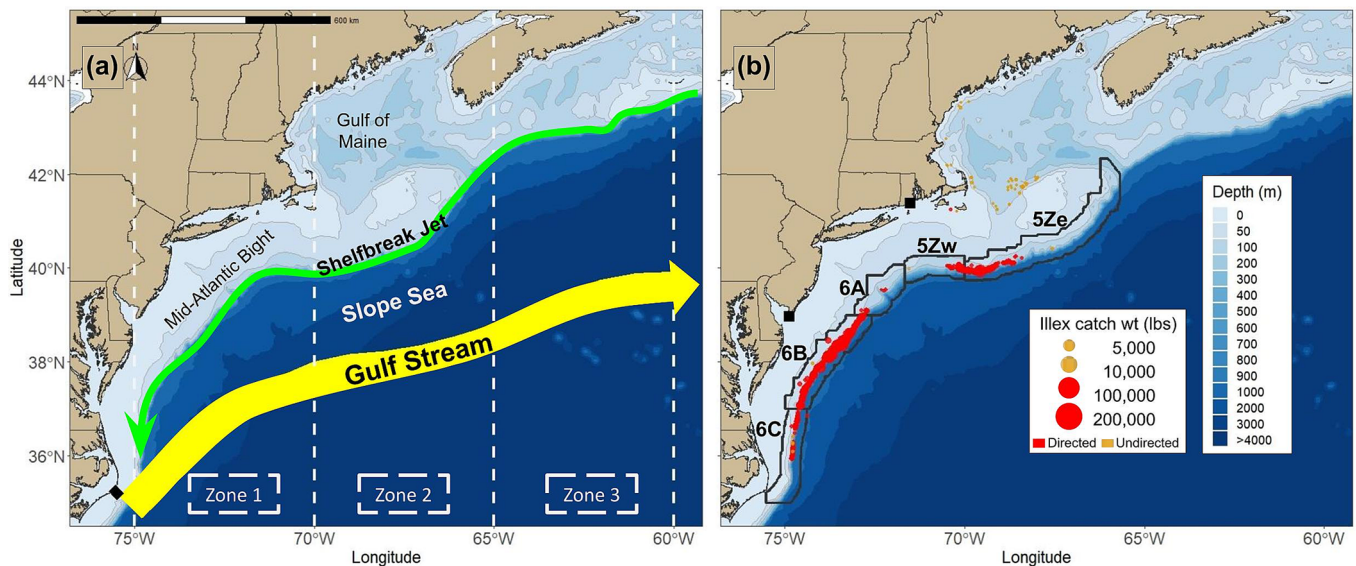
#### KEYWORDS

environmental covariates, generalized additive model, *Illex illecebrosus*, northern shortfin squid, Northwest Atlantic, remote sensing, warm core rings

## 1 | INTRODUCTION

The Northeast US continental shelf (NES) is a large, highly productive, and dynamic marine ecosystem (Sherman & Duda, 1999) that supports multiple major US fisheries, including the northern shortfin squid, *Illex illecebrosus* (hereafter *Illex*). *Illex* is a commercially important, trans-boundary squid inhabiting the continental shelf and slope waters of the Northwest Atlantic Ocean, whose distribution spans from Newfoundland to Florida and crosses the Exclusive Economic Zones (EEZs) of Canada and the United States (Arkhipkin et al., 2015; Hendrickson &

Holmes, 2004; Palacios-Abrantes et al., 2020). The shared US and Canadian stock is split into Northern and Southern stock components for management, by the Northwest Atlantic Fisheries Organization (NAFO) and the Mid-Atlantic Fisheries Management Council (MAFMC), respectively (Hendrickson & Showell, 2019). The US fishery lies within the portion of the Southern stock component associated with the EEZ of the East Coast of the United States (NAFO subareas 5 and 6) and is composed of *Illex* populations extending from the Gulf of Maine to the southernmost portion of the Mid-Atlantic Bight (see Figure 1a; Hendrickson & Showell, 2019; Lowman, Jones, Pessutti, et al., 2021).



**FIGURE 1** (a) Map of Northeast US Continental Shelf Large Marine Ecosystem (NES LME). The Continental Shelf is the water mass located to the west of the shelfbreak (0–200 m, lighter blue colors); the Shelfbreak Jet is the southwardly flowing jet indicated by the green arrow; the Slope Sea is the water mass between the Continental Shelf and the Gulf Stream (>4,000 m); and the Gulf Stream is the northward flowing water mass indicated by the yellow arrow. The filled black square indicates Cape Hatteras, NC. Zone indicates a given region from which the Warm Core Ring Footprint Index (RFI) was derived and consists of longitudinal zones binned by 5° increments (Zone 1: 75–70°W; Zone 2: 70–65°W; Zone 3: 65–60°W). (b) Mean distribution of fishing locations from 2011 to 2020. The size of the point represents the total kept weight of *Illex*, and the color indicates whether the catch was from a directed (red) or undirected trip (orange). Map displays only non-confidential data (weeks with fewer than three permits were removed). For reference, the Northeast Shelf Break (NESBR) region, the spatial scale for multiple covariates, is outlined in black and extends to 40 km on either side of the 200-m isobath. This region is further divided into segments indicating the latitudinal bounds for NAFO subareas (5Ze, 5Zw, 6A, 6B, and 6C). Filled black squares indicate the locations of a northern and southern *Illex* processing facility.

*Illex* is a migratory species whose availability to the US fishery is seasonal and highly variable in space and time. The US fishery is largely confined to the outer edge of the NES and occurs during the late spring through autumn months when squid migrate onto the shelf (Figure 1b). The population variability is driven by the species unique natural history, which includes short life spans (<1 year), high natural mortality, year round spawning, and extreme variability in growth and maturity rates. While many aspects of their life history are still unknown, our current understanding is that the portion of the population that migrates onto the NES is heavily influenced by oceanographic factors (Arkhipkin et al., 2015; Hendrickson, 2004). During early life history stages (eggs, paralarvae), *Illex* are thought to be concentrated in the Slope Sea, the offshore water mass between the continental shelf and the Gulf Stream (GS), and along the North wall of the GS (Figure 1a), whereas juveniles and adults have been associated with the shelf break in the Mid-Atlantic region of the NES (Arkhipkin et al., 2015; Hatanaka et al., 1985; Hendrickson & Holmes, 2004; Perez & O'Dor, 1998). However, due to mismatches in the timing and locations of fisheries surveys and *Illex* distribution, there is a paucity of data describing the full distribution, behaviors of early life-history stages, and precise spawning locations for this species. Thus, because of these large gaps in data, little is known about the offshore and deep water portions of the population that may be migrating onto the shelf (Arkhipkin et al., 2015; Bakun &

Csirke, 1998; Hendrickson, 2004; Hendrickson & Holmes, 2004). Historically, the *Illex* fishery has been defined by high interannual variability in catch; however, in recent years, large increases in *Illex* catch combined with quota constrained fishing seasons have led to early fishery closures occurring in the late summer and early fall months (Hendrickson & Showell, 2019; see Table 1). While specific drivers associated with high abundance years remain unknown, the variable availability of *Illex* to the US fishery is thought to be largely influenced by the dynamic oceanographic conditions of the Northwest Atlantic (Dawe et al., 2007; Hendrickson, 2004; Hendrickson & Holmes, 2004). This notion has elicited increased interest in understanding and identifying which environmental factors may be driving recent increases.

*Illex*'s habitat, the Northwest Atlantic, is a complex and highly variable region subject to oceanic and atmospheric forcing on multiple spatial and temporal scales and is currently undergoing rapid change (Gawarkiewicz et al., 2022; Harden et al., 2020). This region includes multiple water systems, including the NES, Slope Sea, GS, and Shelf-break Jet, which work in concert to drive regional dynamics (Figure 1a). Two major circulation systems, the GS, a warm Northeastern flowing western boundary current, and the cold Southwesterly flowing Shelfbreak Jet (which has a mean position located about the 200 m isobath), stemming from the Labrador Current (LC), meet in the southern portion of the NES around Cape Hatteras, North Carolina

**TABLE 1** Annual descriptions of *Illex* squid cumulative landings for the entire fleet, the combined mean catch for the wet boat fleet within the study fleet (SF), and observer program (OBS), the fishery quota, the date the fishery reached 95% of the quota, and the percentage of the quota that was met by the end of each year (12/31).

Year	Annual landings full Fleet (mt)	Annual catch SF and OBS (mt)	Quota (mt)	95% quota	% quota (entire fleet)
2001	3,831	NA	24,000	NA	16
2002	3,135	NA	24,000	NA	13
2003	7,514	NA	24,000	NA	31
2004	25,913	NA	24,000	09/21	108
2005	11,911	NA	24,000	NA	50
2006	14,144	NA	24,000	NA	59
2007	9,023	NA	24,000	NA	38
2008	15,900	896	24,000	NA	66
2009	18,419	2,298	24,000	NA	77
2010	15,667	2,722	24,000	NA	65
<b>2011</b>	<b>18,795</b>	<b>1,338</b>	<b>23,327</b>	<b>NA</b>	<b>81</b>
<b>2012</b>	<b>11,709</b>	<b>684</b>	<b>22,914</b>	<b>NA</b>	<b>51</b>
<b>2013</b>	<b>3,831</b>	<b>767</b>	<b>22,914</b>	<b>NA</b>	<b>17</b>
<b>2014</b>	<b>8,776</b>	<b>1,898</b>	<b>22,914</b>	<b>NA</b>	<b>38</b>
<b>2015</b>	<b>2,418</b>	<b>673</b>	<b>22,914</b>	<b>NA</b>	<b>11</b>
<b>2016</b>	<b>6,684</b>	<b>957</b>	<b>22,914</b>	<b>NA</b>	<b>29</b>
<b>2017</b>	<b>21,156</b>	<b>8,162</b>	<b>22,914</b>	<b>09/15</b>	<b>98</b>
<b>2018</b>	<b>24,076</b>	<b>8,098</b>	<b>22,914</b>	<b>08/15</b>	<b>105</b>
<b>2019</b>	<b>27,276</b>	<b>9,378</b>	<b>24,825</b>	<b>08/21</b>	<b>109</b>
<b>2020</b>	<b>28,135</b>	<b>4,119</b>	<b>28,643</b>	<b>08/31</b>	<b>98</b>

Note: The US *Illex* fishery closes when 95% DAH is reached, thereby triggering the directed fishery closure. Annual landings and specified quota for *Illex* between years 2001 and 2020; however, the data used in this analysis are restricted to 2011–2020 and are bolded. These data were acquired from the Greater Atlantic Fisheries Office (GARFO) quota monitoring archives ([https://www.greateratlantic.fisheries.noaa.gov/ro/fso/reports/quota\\_monitoring\\_archive.html](https://www.greateratlantic.fisheries.noaa.gov/ro/fso/reports/quota_monitoring_archive.html)).



(35.248°N, -75.5393°W) (Forsyth et al., 2020; Seidov et al., 2021; Townsend et al., 2006). The interplay of these systems results in seasonal and interannual variations in oceanographic conditions influencing the variability in the timing, location, and magnitude of biological and physical features in this region. This, in turn, affects the population dynamics of *Illex* and other commercially important species (Houghton & Visbeck, 1998; Myers & Drinkwater, 1989; Seidov et al., 2021; Townsend et al., 2015). Additionally, this region has experienced significant changes over the past decade (Forsyth et al., 2020; Gonçalves Neto et al., 2021). Most notably, it has been ranked one of the most rapidly warming areas in the World Oceans (Chen et al., 2020; Forsyth et al., 2015; Harden et al., 2020; Pershing et al., 2015) and has been subject to extreme marine heatwaves (Chen et al., 2013; Gawarkiewicz et al., 2019; Großelindemann et al., 2022; Hobday et al., 2016; Perez et al., 2021). Recent work quantifying changes in the region's physical oceanography document shifts in the persistence and extent of the cold pool, a bottom-trapped cold water mass (Chen et al., 2020; du Pontavice et al., 2022), as well as shifts in the location of the GS (Andres, 2016; New et al., 2021; Seidov et al., 2021), and increases in the number and variability of warm core rings (WCRs) and other mesoscale features (Gangopadhyay et al., 2019; Gawarkiewicz et al., 2018, 2022; Harden et al., 2020; Silver et al., 2021). This has resulted in a significant increase in the influence of offshore forcing on the Shelfbreak Front and continental shelf (Gawarkiewicz et al., 2018; Hoarfrost et al., 2019).

Understanding how species respond to the complex and expeditiously changing spatial and temporal variability within this ecosystem is critical for developing effective management strategies. This is particularly true for species associated with the continental shelf break region, as changes in the latitudinal position, strength, and seasonality of the Shelfbreak Front can influence their relative abundance via altered nutrient supplies and resulting effects on primary productivity (Dawe et al., 2007; Drinkwater et al., 2000; Gawarkiewicz et al., 2018). To that end, oceanographic indicators can be used to reflect a variety of physical, chemical, and biological aspects of an ecosystem and provide information on the current state and trends of the system, which can be critical for their assessment and management (Clay et al., 2020; Fu et al., 2012). While the physical and biogeochemical properties of a marine system may show trends across long timescales (e.g., decadal and annual), the changes that occur on short timescales (e.g., sub-seasonal; weekly and monthly) can have large impacts on a stock's availability to fisheries. Therefore, identifying oceanographic indicators at ecologically relevant scales is key to gaining insights into the spatiotemporal distribution of marine species. This is particularly critical for short-lived species, like *Illex*, whose availability and distribution exhibit high variability on sub-annual time scales (Dawe & Beck, 1997).

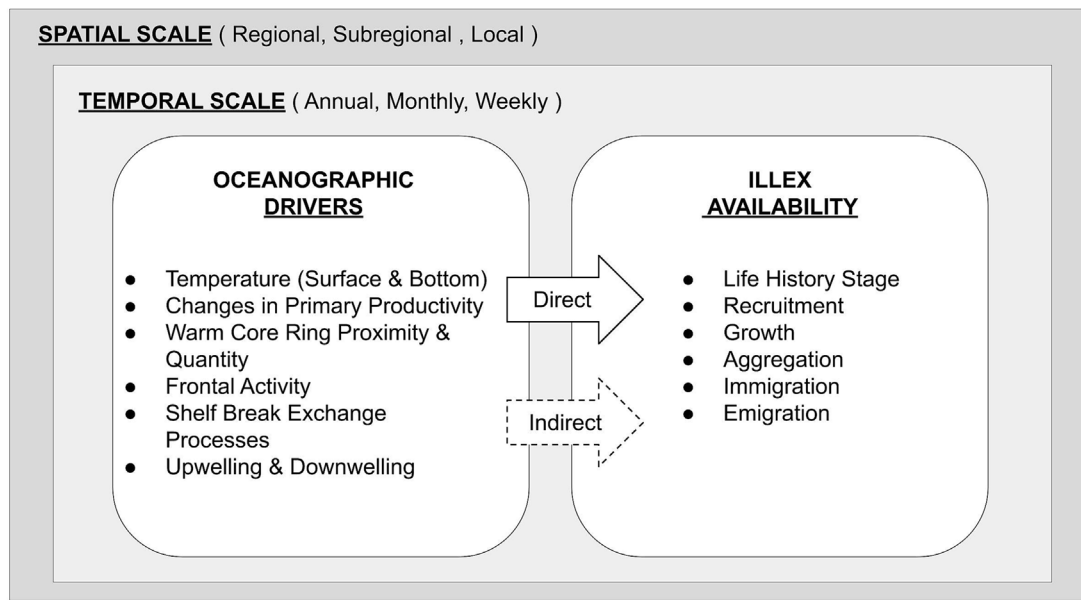
Satellite remote sensing data are a powerful tool for developing oceanographic indicators as they provide reliable synoptic coverage of oceanographic variables, such as sea surface temperature (SST) or ocean color (i.e. chlorophyll), at spatial (1–4 km) and temporal (~daily) resolutions not attainable by in situ sampling. Furthermore, these data can be used to identify oceanographic features such as fronts or

eddies (Miller et al., 2015; Silva et al., 2020), monitor the variability of phytoplankton biomass, production and composition (Turner et al., 2021), and evaluate the spatial patterns of higher trophic level animals relative to these features (Miller & Christodoulou, 2014; Polovina & Howell, 2005; Saba et al., 2015). We used long-term satellite time series, as well as global ocean reanalysis physical data, to generate high-resolution metrics, including the location of frontal gradients and mesoscale eddies at weekly time scales. Specifically, this study investigated a suite of oceanographic features to assess and characterize their relationships to *Illex* catch rates. To achieve this goal, we collaborated with a multi-disciplinary group of experts across government, academia, industry, and management to generate a series of hypotheses (see Section 2.1) linking oceanographic features (e.g., WCRs, shelf streamers, and Shelfbreak Jet) to potential mechanisms driving both the ingress and egress of *Illex* to the US fishery. The identification of oceanographic drivers of *Illex* catch in space and time is an important first step in increasing our understanding around potential mechanistic processes influencing the movement of this species and is highly relevant for reaching future stock assessment and management goals for *Illex*.

## 2 | MATERIALS AND METHODS

### 2.1 | Conceptual model

In an effort to isolate important environmental variables to serve as oceanographic indicators of *Illex* availability, our interdisciplinary team developed a conceptual model (Figure 2), to link candidate variables at their relevant spatiotemporal scales to *Illex* life history characteristics. Conceptual models are useful tools for integrating and organizing knowledge from diverse experts into a unified framework (Levin et al., 2016), specifying the linkages between potential quantitative models and available data (DePiper et al., 2017), and help focus modeling efforts on key interactions (e.g., Haltuch et al., 2020; Tolimieri et al., 2018). We refined the model by identifying direct and indirect links between environmental variables and life history characteristics. From there, we developed general hypotheses identifying potential oceanographic drivers of important *Illex* biological processes including growth, mortality, immigration, emigration, and aggregation. We derived the following set of assumptions via a combination of existing theories in the literature and original ideas to describe how oceanographic influences could affect habitat conditions and food resources for this species: (1) bottom temperatures influence habitat selection for managing metabolic demands of juveniles and adults (Benoit-Bird & Moline, 2021); (2) frontal dynamics create areas of high primary productivity (Belkin & O'Reilly, 2009; Bost et al., 2009); (3) WCRs serve as a transport/retention mechanisms for paralarval stage/pre-recruits; (4) the strength and location of WCRs contribute to increased primary productivity due to upwelling of nutrients (Forsyth et al., 2022), providing a mechanism to concentrate food sources for juveniles and adults; and (5) changes in shelf and slope water composition impact the spatial distribution of *Illex*. Thinking



**FIGURE 2** Schematic of the conceptual model. This is a preliminary version of the conceptual model developed to outline the oceanographic drivers and their associated spatial and temporal scales. In the final version of the conceptual model, each variable was identified at the spatial and temporal scale in which it was most likely to influence a particular aspect of *Illex* life history. Connections between drivers and availability were marked as either direct (solid lines) or indirect (dashed lines).

through the relationships detailed in the conceptual model informed the selection and spatiotemporal scale of covariates considered for the statistical models used in this study (Figure 1; Table S2.1). Thus, the conceptual model served as an initial variable selection step, as we prioritized the variables underlying the assumptions stated above and the resulting covariates were fed into a generalized additive model (GAM). While we could not directly test these hypotheses due to data limitations, conceptualizing the drivers in this way allowed us to tailor our variable selection to examine oceanographic indicators with higher relevance *Illex* availability.

## 2.2 | Fishery dependent catch data

### 2.2.1 | Data sources

This study uses nominal *Illex* catch per unit effort (CPUE) calculated from two high resolution fishery-dependent data sets maintained by the Northeast Fisheries Science Center's (NEFSC) Study Fleet and Observer programs (Jones et al., 2022; Palmer et al., 2016). NEFSC independent bottom trawl survey data was considered, but it was ultimately excluded due to the mismatch between the timing and location of the surveys and the instances when *Illex* are present on the continental shelf, due to migration patterns. While this species constitutes a single stock throughout its range, the catch data used in these analyses are derived solely from the US Domestic Fishery (the Southern stock component, in NAFO subareas 5 and 6; see Figure 1). We selected the Study Fleet and Observer datasets for this study as they provided the fine scale spatiotemporal data on *Illex* catch and effort

required for exploring oceanographic drivers of *Illex* availability. Specifically, these datasets include detailed fishing location start and end points for individual tows via GPS coordinates, which was instrumental for pairing with co-located environmental conditions. The Study Fleet data are voluntary, self-reported catch, and effort data from individual tows collected by captains on participating vessels, from 2008 to present (Jones et al., 2022). The Study Fleet data are collected from ~40% of *Illex* fishing trips annually, with higher coverage in recent years. The Observer program dataset consists of catch data collected per tow, onboard commercial fishing vessels by professionally trained biologists (observers) during a subset of randomly selected *Illex* fishing trips. This data set ranges from 1989 to present and is collected from approximately 10% of the *Illex* fishing trips annually, with lower coverage rates in recent years. While these data represent a subset of the entire *Illex* fishing fleet, recent research indicates that the Study Fleet/Observer data sets are representative of the overall *Illex* fleet(s) (Jones et al., 2020, 2022; Mercer et al., 2022).

### 2.2.2 | Metrics calculated

The CPUE was calculated as the weight of *Illex* caught divided by the duration of the tow (lbs/h) for each individual tow. The resulting values were summed across weeks and fishing locations. Models run in this study utilize catch from both directed *Illex* fishing trips (where *Illex* was the target species) and undirected fishing trips (where *Illex* was incidental catch) from vessels using bottom trawl gear, in an effort to reduce the biases implicit in using fishery dependent catch and effort data as an index of abundance (Harley et al., 2001). Here,

directed trips are fishing trips where more than 50% of the total catch is comprised of *Illex* and more than 10,000 pounds (4,535 kg) were landed (NEFSC, 2006), whereas undirected trips are fishing trips with lower *Illex* landings, where *Illex* comprises between 10% and 50% of total catch and more than 100 pounds (45 kg) landed. Using this comprehensive set of *Illex* catch data allowed for the examination of a larger number of trips over a greater range of space and time and enabled us to capture instances of both low and high catch throughout the region. Including instances of low catch allowed us to explore a wider swath of the distribution, accounting for areas where *Illex* may be present, yet not sufficiently aggregated for commercial fishing purposes. The resulting catch data were subset into two fishing fleets based on vessel hold type (freezer trawlers and “wet boats”). Freezer trawlers are vessels with the capacity to freeze catch on site, whereas “wet boats” is a term used for vessels with either refrigerated sea water or ice holds. This decision follows work by Lowman, Jones, Pessutti, et al. (2021) as well as correspondence via *Illex* Working Group meetings and industry conversations, where clear differences in fishing behavior and capacity were noted between fleets (Mercer et al., 2022). These differences stem from the highly perishable nature of this species and differential processing capacity of the two fleet types (Lowman, Jones, Pessutti, et al., 2021; Mercer et al., 2022). For instance, to prevent product from spoiling, wet boats face constraints around steam time and fishing location, which makes them more likely to adjust fishing behavior in response to squid abundance and oceanographic conditions. Thus, these vessels are more apt to target dense squid aggregations associated with oceanographic features as opposed to freezer trawlers, whose ability to freeze catch at sea allows them to exhibit more consistent fishing behavior over longer fishing trips. Furthermore, the fishing activity of freezer trawlers is limited by at-sea freezing, which could dampen signals in the catch rates. Finally, “wet boats” make up the majority of the *Illex* fishing fleet (>90%). In effort to identify oceanographic indicators of *Illex* availability, we focused these analyses on wet boat catch rates, as they were most likely to be connected to oceanographic dynamics and most representative of the fishing fleet.

## 2.3 | Oceanographic covariate data

### 2.3.1 | Data sources

The majority of the environmental covariates were either, direct observations via remotely sensed satellite imagery, or derived from a global physical reanalysis model.

#### *Remote sensing data*

Daily Level 3 (L3) satellite ocean color data (version 5.0; Sathyendranath et al., 2021) were obtained from the European Space Agency's Ocean Colour Climate Change Initiative (OC-CCI) project (Sathyendranath et al., 2019). Daily Level 4 (L4) interpolated SST data were acquired from the Group for High Resolution Sea Surface Temperature (GHRST) Multiscale Ultrahigh Resolution (MUR, version 4.1) data

(JPL MUR MEaSUREs Project, 2015; Chin et al., 2017). The global CHL and SST products were gridded and spatially subset to the US East Coast (SW longitude =  $-82.5$ , SW latitude =  $22.5$ , NE longitude =  $-51.5$ , NE latitude =  $48.5$ ). We derived weekly statistics (minimum, maximum, mean, standard deviation, and coefficient of variation) for both CHL and SST. Additionally, the climatological weekly means were calculated from the entire time series (1998–2020 for CHL and 2003–2020 for SST) to generate anomalies (see Appendix S1 for details). Daily high resolution (1 km) MODIS imagery from the Aqua and Terra satellites acquired from the NASA Ocean Biology Processing Group (OBPG) were used to calculate frontal metrics (see the Oceanographic Fronts section below and Appendix S1 for more details).

#### *Global ocean reanalysis model data*

Subsurface salinity and bottom temperature time series were obtained from the GLobal Ocean ReanalY-sis and Simulation project (GLORYS12V1) global ocean reanalysis model (CMEMS, 2018), which is a global ocean, eddy-resolving, and data assimilated hindcast from Mercator Ocean (Chen et al., 2021; du Pontavice et al., 2022). The global data were subset over the same Northwest Atlantic region as the satellite imagery and averaged to create weekly products. The reanalysis product has a gridded 8-km horizontal resolution, up to 50 fixed vertical depth bins, and the data are available from 1993 to 2020 (Fernandez & Lellouche, 2018; Lellouche et al., 2021).

### 2.3.2 | Metrics calculated

#### *Oceanographic fronts*

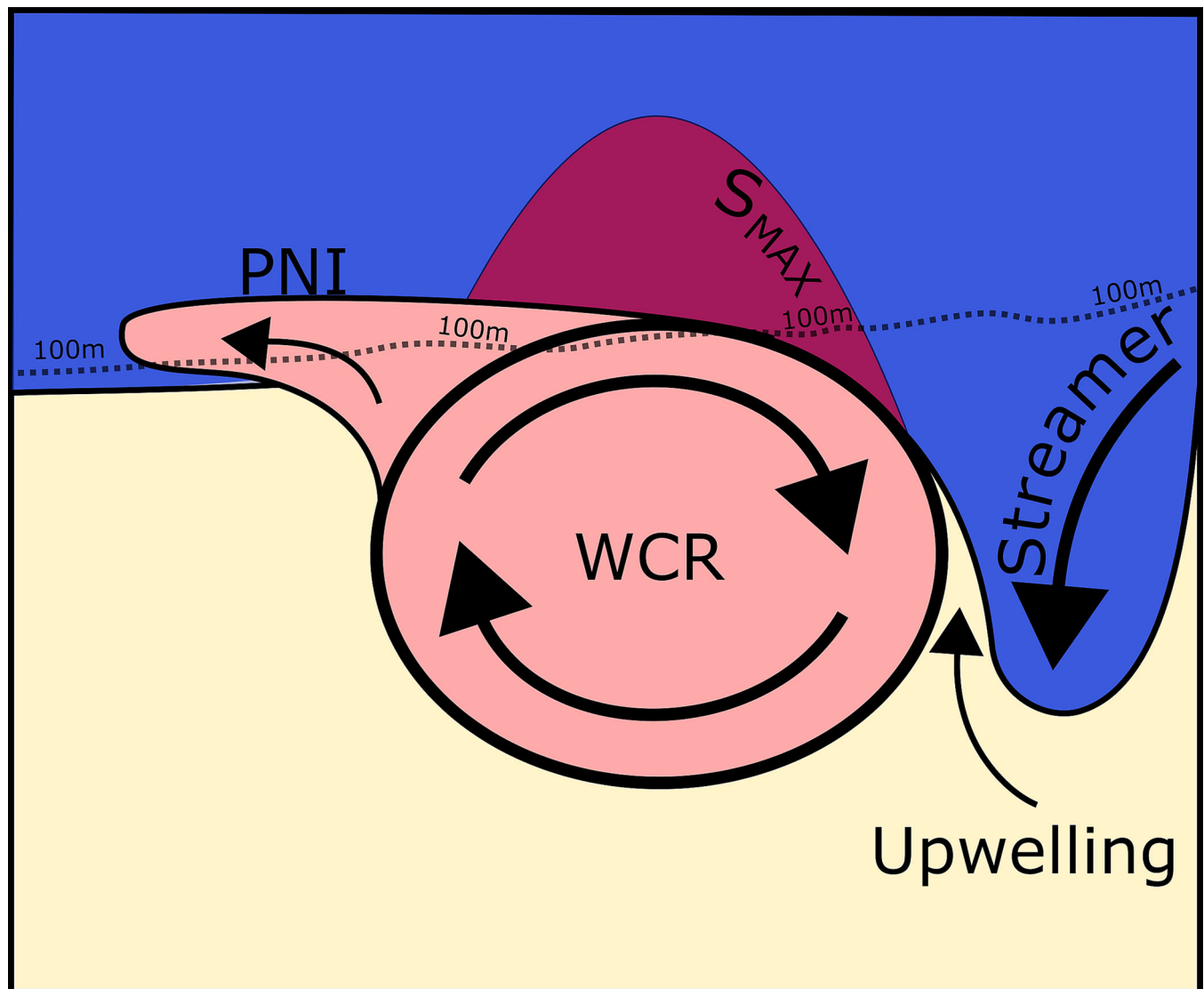
Oceanographic fronts are narrow zones of enhanced horizontal gradients of water properties (temperature, density, chlorophyll, etc.) that represent major biogeographical boundaries and are often associated with zones of elevated primary and secondary productivity, in turn, creating “hot spots” of marine life and fishing (Belkin & O'Reilly, 2009; Bost et al., 2009; Miller et al., 2015). We used daily high resolution (1 km) MODIS imagery from the Aqua and Terra satellites acquired from the NASA OBPG to calculate daily SST and CHL frontal gradients using the Belkin and O'Reilly (2009) algorithm. The gradient data are normalized differences between pixels; therefore, data from the Aqua and Terra sensors were merged into daily files, which were then used to create weekly frontal metrics. In order to isolate prominent frontal features, thresholds of  $.4^{\circ}\text{C}$  for SST and  $.06\text{ mg m}^{-3}$  for CHL were applied to the frontal gradient data (Miller, 2009; Suberg et al., 2019). We then identified the number of valid frontal pixels by summing the number of times a pixel exceeded the frontal threshold across a 7-day period (Suberg et al., 2019). For example, if a pixel was identified as a front on days 1, 3, 4, and 5 of a given week, it would have a frontal value of 4. Note the percentage of “clear” days (i.e., days without clouds) were not factored into this metric; thus, a week with six cloudy days and only 1 day with an observed front would have a value of 1. The final frontal index, the proportion of frontal pixels in a given subarea at a weekly resolution, was

calculated by tallying the total frontal values and averaging across each subarea within the Northeast Shelf Break (NESBR; see Table S2.1 and Figure 1 for details on areas of data extraction). This index was generated in effort to represent frontal dynamics across the spatial range of the US fishery.

#### WCR metrics

WCRs are anticyclonic mesoscale eddies that break off from the GS, after it moves away from the coast downstream of Cape Hatteras (Joyce, 1984, 1985). Once detached from the stream, these mesoscale eddies move in a west-southwestward direction carrying the

entrapped warm GS water through the Slope Sea to the US continental shelf region (Gangopadhyay et al., 2020; Silva et al., 2020). When a WCR impinges on the sloping bathymetry (Figure 3), its inherent anticyclonic properties (clockwise movement of surface waters) create different shelf break exchange processes on opposing sides of the ring (Cenedese et al., 2013; Gawarkiewicz et al., 2018; Morgan & Bishop, 1977). On the eastern edge of the ring where the ring circulation moves away from the shelf, the productive, cooler, and less saline shelf water is entrained and exported into the Slope Sea, creating a “streamer” of shelf water (Bisagni, 1983; Gawarkiewicz et al., 2001). These shelf water streamers interact with the Mid-Atlantic Bight



**FIGURE 3** Depiction of warm core ring (WCR) impingement on the shelf sloping bathymetry and the associated physical processes. Due to the WCRs anticyclonic flow, the western, leading edge of the ring, works to move warm, saline surface waters onshore towards the shelf. This can result in an along-isobath intrusion of warm water called a Pinocchio's Nose Intrusion (PNI), which can extend 100 s of kilometers along the shelfbreak (Zhang & Gawarkiewicz, 2015). Conversely, on the eastern, trailing edge of the ring, the circulation moves water away from the shelf, entraining and exporting productive, cooler, and less saline shelf water into the Slope Sea, creating a “streamer” of shelf water (Forsyth et al., 2022). Shelf water streamers can interact with the subsurface Shelfbreak Jet, resulting in an area of divergence and increased upwelling. Mid depth salinity maximum intrusions (Smax) are another important feature that can form off WCRs (Gawarkiewicz et al., 2022). These occur where warm saline slope/ring water intrudes on to the continental shelf generally along the seasonal pycnocline.

(MAB) Shelfbreak Jet resulting in an area of divergence and increased upwelling (Forsyth et al., 2020, 2022; Ryan et al., 1999). Conversely on the western edge of the ring where the ring circulation moves toward the shelf, steepening of the Shelfbreak Front combined with an onshore flow, results in warmer, more saline Slope Sea and ring water intrusions (Gawarkiewicz et al., 2001). The significant increase in the number and frequency of mesoscale eddies (Gangopadhyay et al., 2019) and Slope Sea intrusions (Gawarkiewicz et al., 2022) may be a key component in the changing dynamics of the Northwest Atlantic shelf and slope water ecosystems (Bisagni et al., 2019; Chen et al., 2020; Gawarkiewicz et al., 2018; Harden et al., 2020). We calculated a series of metrics in order to quantify which aspects of a WCR may be influencing *Illex* population dynamics.

#### i. Ring tracking census

First, a GS ring tracking dataset of weekly ring size and location was generated from Jenifer Clark's GS Charts for the years 2011 through 2020 (Silver et al., 2022). These charts provided the data to create a 38-year WCR census (Gangopadhyay et al., 2019, 2020). Following the same methodology as in Gangopadhyay et al. (2020), location and ring area were verified using a Geographic Information System QGIS framework (QGIS Development Team, 2016). Several different ring indices were created from this dataset.

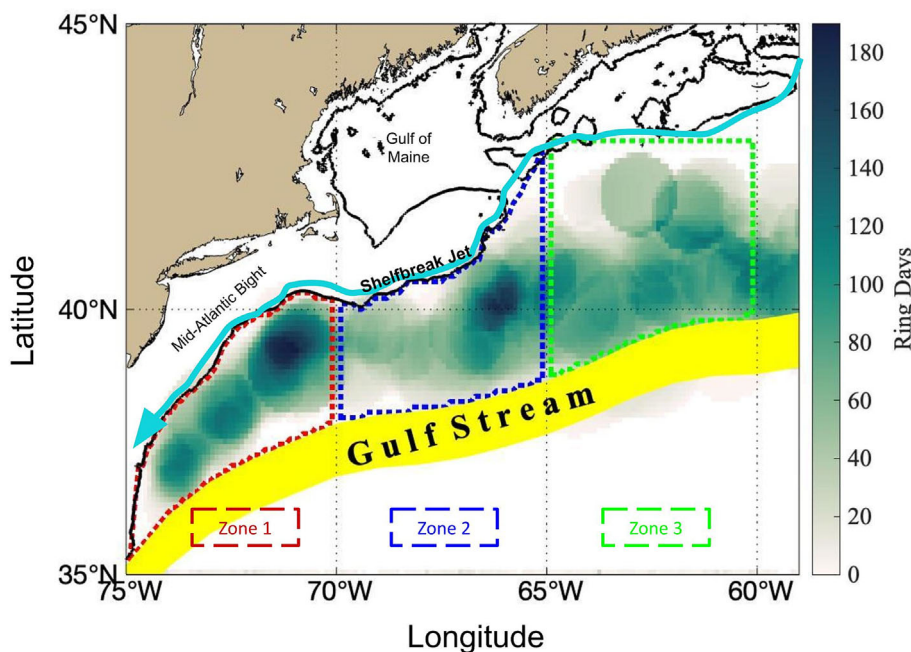
#### ii. Ring Footprint Index

The Ring Footprint Index (RFI) accounts for both the amount of time a ring spends in a given area as well as its size. It is defined as the fraction of time and space that rings occupy in the Slope Sea in a given time period (month or year) in a specific region (a box or a zone as in Figure 1), so  $RFI = \sum \text{ring days per ring area} /$

$(\text{total area of region} * \text{total time period})$ . This index was adapted from the RFI calculated in Gangopadhyay et al. (2020). The numerator,  $\sum \text{ring days per ring area}$ , multiplies the time a ring is in a given region (zone) by the area of the ring and adds all such “ring days times ring area” in that region. This term is then divided by a second term, which multiplies the total area of the zone by the total time period of interest. This was calculated at a weekly time scale across four different longitudinal zones binned by 5° increments (Zone 1: 75–70°W, Zone 2: 70–65°W, Zone 3: 65–60°W; see Figure 4). Additionally, as WCRs in these zones generally move in a southwesterly direction (towards the shelf break), we were able to implement ecologically relevant time lags to better understand the timing of ring conditions and examine the potential for transport that could arise ahead of the summer fishery.

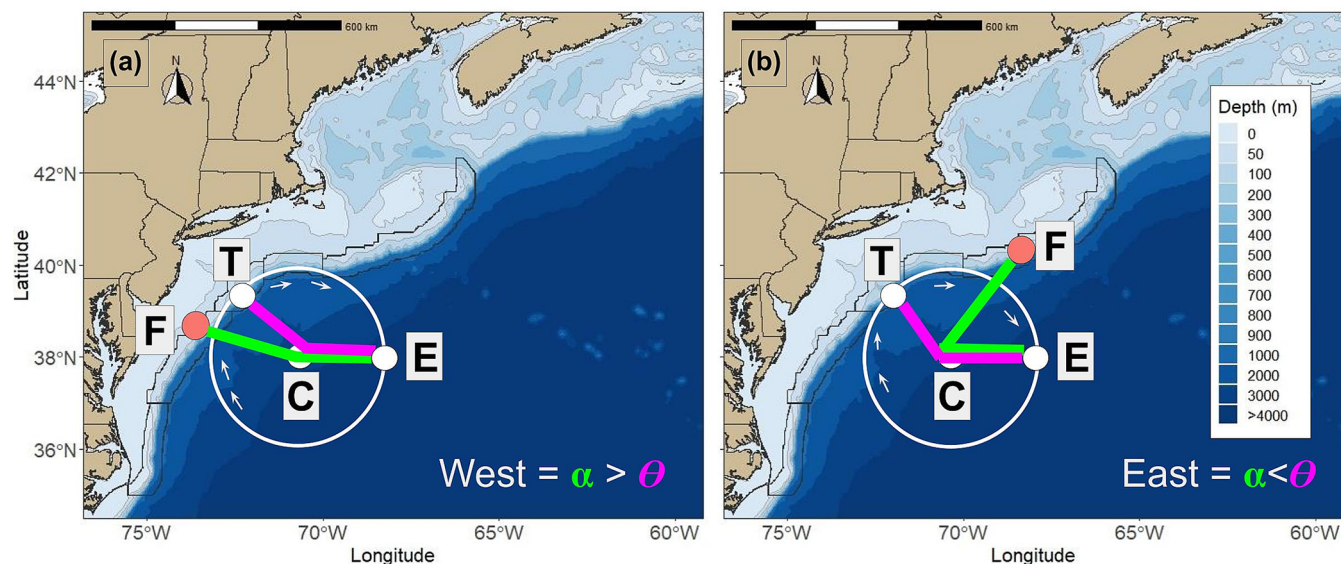
#### iii. Ring Orientation

Ring Orientation describes the relationship between the physical properties of WCRs and catch locations. Quantifying the orientation of a WCR to a fishing location can provide information about the oceanographic processes and associated ecological implications related to the presence of a ring. For a given week, we calculated the distance between individual fishing points and all rings present. Ring orientation was then calculated as the angle between a given fishing point and the closest ring associated with that location (Figure 5). Specifically, coordinates detailing each ring's northern, western, eastern (E), southern, and center (C) points were identified, along with the location (T) at which the ring meets the 100 m isobath, which is the approximate position of the shelf break. This series of coordinates was then paired with fishing locations (F) and used to generate two lines and their associated angles (Figure 5). Theta ( $\theta$ ,  $\angle TCE$ ) is the angle formed from lines (TC) and (CE), which are calculated from the



**FIGURE 4** Heat map of Ring Footprint Index (RFI). The blue southward pointing arrow indicates the Shelfbreak Jet. The yellow band indicates the mean position of the Gulf Stream North Wall. The color bar represents the number of ring days in 0.1° bins ranging from 0 to 200. Vertical bars represent the region (zone) from which the RFI was derived, where Zone 1 is indicated in red and spans 75–70°W, Zone 2 is indicated in blue and spans 70–65°W, and Zone 3 is indicated in green and spans 65–60°W. The bathymetry line represents the 100 m isobath and demarks the approximate location of the shelf break.





**FIGURE 5** Depiction of warm core ring impingement on the shelf slope and derivation of ring orientation. The bathymetry lines depict depths ranging from 0 to >4000 m. The white circle in both panels (a, b) represents a warm core ring, and the small white arrows inside the ring indicate the direction of circulation associated with an anticyclonic eddy. The location where the ring meets the Shelfbreak is the 100 m isobath. The reference points on the ring are (T = the location where the ring meets the 100 m isobath, C = center of point of ring, E = eastern point of ring). The orange circle (F) indicates a fishing point location. (a) The western side of the ring is associated with onshore intrusions. (b) The eastern side of the ring is associated with offshore transport processes that lead to upwelling. The lines TC and CE represent the ring location in relation to the shelf and form the (purple) angle theta (TCE,  $\theta$ ). Lines FC and CE detail the fishing point location in relation to the nearest ring and form the (green) angle (FCE,  $\alpha$ ). When alpha ( $\alpha$ , FCE) is greater than theta ( $\theta$ , TCE), the ring has a western orientation to the fishing point. Conversely, when angle alpha ( $\alpha$ ) is less than angle theta ( $\theta$ ), the ring is oriented to the east of the fishing point.

lines describing locations between where the ring impinges on the shelf to its center and from the center of the ring to the Eastern point (E) of the ring. Alpha ( $\alpha$ ,  $\angle FCE$ ) is the angle formed from lines (FC) and (CE), which delineate the location of the fishing point to the center of the nearest ring and the center of the ring to the Eastern point of the ring.

$$\theta = \arctangent(T_{lat} - C_{lat}, T_{lon} - C_{lon}) * \frac{180}{\pi} - \arctangent(C_{lat} - E_{lat}, C_{lon} - E_{lon}) * 180/\pi$$

$$\alpha = \arctangent(F_{lat} - C_{lat}, F_{lon} - C_{lon}) * \frac{180}{\pi} - \arctangent(C_{lat} - E_{lat}, C_{lon} - E_{lon}) * 180/\pi$$

Comparison between resulting angles was used to determine the orientation of a given ring to individual fishing locations. Specifically, in instances where alpha ( $\alpha$ ,  $\angle FCE$ ) was greater than theta ( $\theta$ ,  $\angle TCE$ ), the fishing point was oriented to the West of the ring. Conversely, when angle alpha ( $\alpha$ ) was less than angle theta ( $\theta$ ), the fishing point was oriented to the East of the ring.

The fishery-dependent catch data and oceanographic metrics used for this study were truncated to a common 10-year time period (2011–2020) for which fine-scale WCR tracking data were available.

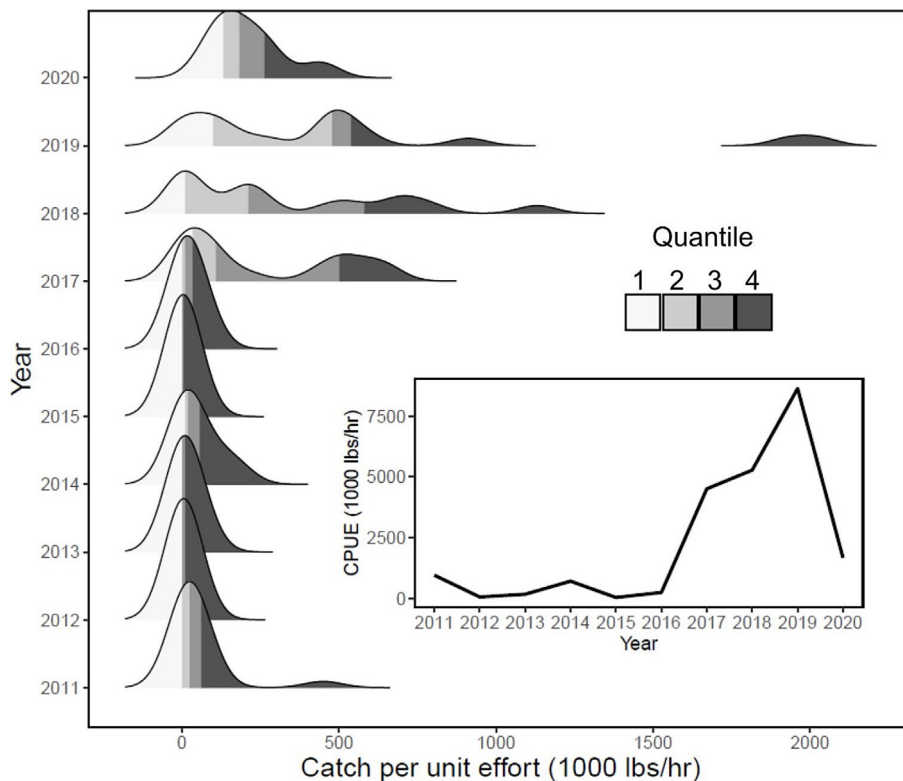
## 2.4 | Data analysis

### 2.4.1 | Inter-annual variability of *Illex* catch and distribution of fishing

To test differences in annual catch between years, we summed the total catch from the combined Study Fleet and Observer data sets and performed the nonparametric Kruskal-Wallis test. To explore the inter-annual differences in catch availability, we conducted pairwise comparisons using Dunn's test with a Bonferroni adjustment. We used a ridge plot with quantile analysis to visualize the inter-annual variability in the distribution of fishing (Figure 6).

### 2.4.2 | Generalized additive modeling

To examine relationships between *Illex* CPUE and oceanographic covariates, we fit GAMs to the combined Study Fleet and Observer data-sets. GAMs, an extension of General Linear Models (GLMs), are a powerful statistical tool that is increasingly used in ecological contexts as they are inherently flexible and thus able to account for nonlinear relationships without compromising interpretability (Pedersen et al., 2019; Wood, 2011). This flexibility stems from the additive framework of GAMs, which uses local smoothing functions to fit



**FIGURE 6** Catch per-unit effort over time for the Study Fleet and Observer Program wet boat fleet from 2011 to 2020. The inset figure is a time series of CPUE. The main figure details the density distributions of annual catch-per-unit effort across years. Each distribution is partitioned into four quartiles, delineated by an increasing gray scale, with lower quartile values represented in white and the darkest gray representing values in the upper quartile.

predictor variables to a response variable. For our models, the response variable (CPUE) was assumed to follow a negative binomial distribution with a log link function to account for positive skew and over dispersion. Predictor variables consisted of 31 candidate oceanographic metrics selected from the conceptual model at ecologically relevant spatial scales (see Appendix S2; Table S2.1). We tested for collinearity among predictor variables via Spearman's rank correlation and variance inflation factor analyses and eliminated predictors with high values ( $\rho > .4$ ,  $VIF > 4$ ; see Tables S2.2 and S2.3). Thin-plate regression splines were used as smoothers to model main effects, with the exception of "Week," which was modeled as cyclic cubic spline to account for periodicity. Models were trained on a subset of the full data set using a simple training/testing data splitting algorithm, selecting 70% of the data to be used for training with the remaining 30% retained for analysis. Model residuals were examined for significant autocorrelation, and we found a general absence of autocorrelation (Appendix S2; Figure S2.2). GAMs were fit using explicit models representing different variations of our previously established hypotheses about how the system works. The optimal model was chosen based on selection criteria that favored the lowest Akaike Information Criterion (Anderson & Burnham, 2004; Brodziak & Walsh, 2013) and highest deviance explained. The optimal model was defined as

$$\begin{aligned} \text{CPUE} \sim & f(\text{lat}, \text{lon}, k = 25) + f(\text{year}, \text{week}, k = c(5, 5)) + f(\text{year}, k = 5) \\ & + f(\text{week}, k = 5) + f(\text{bottom temperature}, k = 4) \\ & + f(\text{salinity}222\text{m}, k = 5) + f(\text{zone}2\text{lag}6\text{mo}, k = 5) \\ & + f(\text{zone}1\text{lag}3\text{mo}, k = 5) + f(\text{zone}3\text{lag}6\text{mo}, k = 5) \\ & + f(\text{fvalid}_{\text{CHL}}, k = 5) + f(\text{sst}_{\text{sd}}) + \text{ORIENTATION}. \end{aligned}$$

Since we were working with limited data, reasonably small  $k$  values were selected to prevent overfitting and aid in interpretation. All GAMs and subsequent analyses were run in R 4.0.5 (R Core Team, 2021) using the *mgcv* package (Wood, 2011, 2017).

### 3 | RESULTS

#### 3.1 | Inter-annual distribution of catch locations

There was a significant influence of year on annual CPUE in the Study Fleet and Observer datasets ( $H[12] = 1,765.5$ ,  $p < .001$ ; Figure 6). Pairwise comparisons using Dunn's test with a Bonferroni adjustment indicated that total *Illex* catch during recent years (2017–2020) was significantly higher than total *Illex* catch reported from 2008 to 2016 ( $p < .001$ ; Figure 6). There is a shift in the median catch per-unit effort and increased variability in the maximum catch for the last 4 years of the data set (2017–2020) as compared to the previous 6 years (2011–2016).

#### 3.2 | Generalized additive modeling (catch data)

GAM results identified 12 covariates that were important predictors of *Illex* catch-per-unit-effort, including temporal (year and week), spatial (latitude and longitude), and environmental (bottom temperature, RFI at various time lags, ring orientation, salinity at 222 m depth, chlorophyll frontal activity, and standard deviation in SST) variables

(Table 2; Figure 7). The full model accounted for 56.2% of the deviance explained. Model predictions using the testing dataset closely followed the model data (Figure 8). While there is evidence of slight overfitting, the final model had fairly good predictive ability ( $RMSE_{\text{actual}}: .06, RMSE_{\text{predict}}: .08$ ).

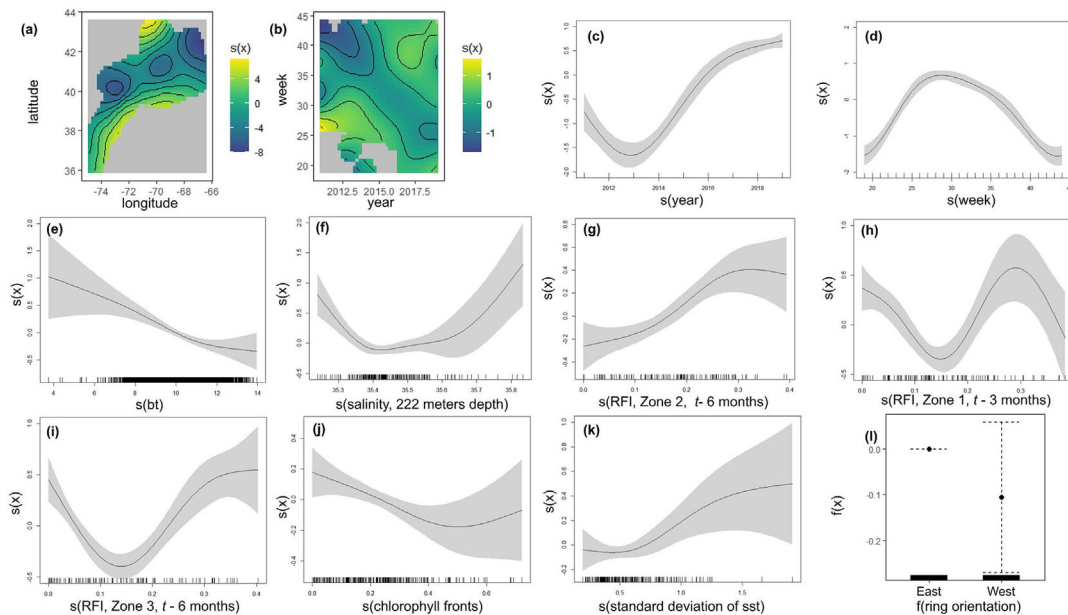
### 3.2.1 | Spatiotemporal trends

The spatial smoother captured the interacting effects of latitude and longitude and identified two hot spots of catch along the Northern and Southern portions of the shelf break (Figure 7a). The main

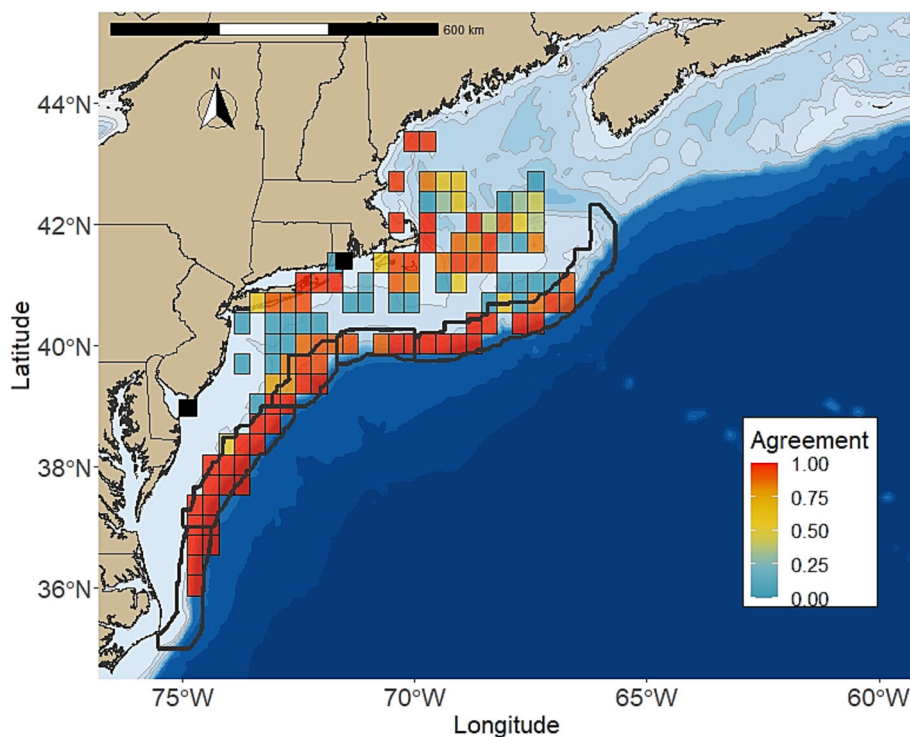
**TABLE 2** Generalized additive model (GAM) results for final model smooth terms in relation to catch-per-unit-effort (CPUE)

Parametric coefficients	Estimate	Std. error	t value	p value
Intercept	7.02597	.04962	141.604	<.0001
Orientation(W)	-.10613	.08399	-1.264	.206
Smooth terms	edf	Ref.df	Chi.sq	p value
s(lon,lat)	22.306	24	3,110.610	<.0001
ti(year,week)	10.613	12	98.273	<.0001
s(year)	3.707	4	232.362	<.0001
s(week)	2.869	3	172.712	<.0001
s(bt)	1.936	3	23.923	<.0001
s(sal_222m)	2.526	4	23.187	<.0001
s(z2lag6mo)	1.947	4	23.298	<.0001
s(z1lag3mo)	3.702	4	37.903	<.0001
s(z3lag6mo)	3.414	4	49.069	<.0001
s(fvalid_chl)	1.527	4	8.123	.00336
s(sst_sd_shbr)	1.669	4	8.687	.00336

Note: Final model accounted for 56.2% of deviance explained. Parametric coefficients are listed in Appendix S2.



**FIGURE 7** Generalized additive model (GAM) partial residual plots for variables with significant relationships to catch per unit effort (CPUE). Covariates are plotted against their splines (held constant); thus, the y axis represents changes in CPUE (the response variable) relative to its mean. The black tick marks inset along the x axis of each plot are the actual values of each variable. The gray shaded region flanking each smooth is the 95% confidence interval for the mean shape of the effect. Smooths are presented in order of the strength of their relationship to CPUE: (a) latitude/longitude; (b) year/week; (c) year; (d) week; (e) bottom temperature; (f) salinity at 222 m depth; (g) Ring Footprint Index in Zone 2, lagged by 6 months; (h) Ring Footprint Index in Zone 1, lagged by 3 months; (i) Ring Footprint Index in zone 3, lagged by 6 months; (j) chlorophyll frontal activity; and (k) standard deviation of SST. The last panel shows the factor (j) ring orientation.



**FIGURE 8** Model predictive ability. Predicted values calculated from the testing data set, comprised 30% of the complete data set. Actual values are CPUE values from the training dataset, which comprised 70% of the complete dataset. The ratio between the actual and predicted values was calculated, and the color bar represents those ratios along a gradient from warm colors, where 1 is total agreement to cooler colors, where 0 is no agreement.

temporal trends that emerged in the full model are consistent with findings from Jones et al. (2022) as well as Lowman, Jones, and Mercer (2021), where catch is relatively stable in the beginning of the time series (2011 and 2012), experiences a drop in year 2013 followed by three consecutive low years (2014, 2015, and 2016), and higher catch over the most recent 4 years (2017, 2018, 2019, and 2020; Figure 7b,c). There is a strong effect of week as well, with the majority of catch associated with weeks 26 through 36 (Figure 7d), suggesting a strong seasonal effect. There is, however, interannual variability in the weekly trend, where the bulk of catch occurs in the early weeks of the fishing season during the first few years in the time series (2011–2013) and a second peak in catch occurs later in the fishing season during the most recent, high yield years (2017–2020) (Figure 7b).

### 3.2.2 | Environmental trends

The ecological predictors of the most parsimonious model revealed informative patterns. The most impactful ecological predictor in this analysis was bottom water temperature. Its effects suggest a small range of cooler bottom temperatures (6–10°C) support higher catch (Figure 7e). Salinity at 222 m depth exhibits an increasing relationship between salinity and catch at values greater than 35.4 (Figure 7f). The mesoscale features that were significant included the RFI, a measure of ring occupancy in the Slope Sea, within all three zones (see Figure 1) at various time lags. Nonlinear relationships between CPUE and ring occupancy emerged in Zone 2 (70–65°W), Zone 1 (75–

70°W), and Zone 3 (65–60°W) at 6 and 3 months prior to catch (Figure 7g,h,i). For each zone, peak catch occurs when WCRs account for approximately 30% of the area in a given week (Figure 7g,h,i). Additionally, there was a negative effect of ring orientation on *Illex* catch, where fishing locations oriented on the western side of WCRs were generally associated with lower catch than fishing locations on the eastern side of rings (Figure 7j). There was a slight increase in CPUE when chlorophyll fronts occupy proportions of the shelfbreak region between .25 and .35 (Figure 7j). However, while the maximum proportion of the region that constituted a chlorophyll front was .72 (see Appendix S2; Table S2.1), the sample size decreases a great deal for values beyond .4. Therefore, it is difficult to interpret trends when chlorophyll fronts occupy proportions of the area that exceeding .4. Finally, the fitted curves in Figure 7k show that increased variability of SST (larger standard deviation values) is a significant predictor of CPUE.

## 4 | DISCUSSION

The results from this study largely support the hypotheses derived by the multidisciplinary research team during the development of the conceptual model. In particular, the results indicate a suite of environmental variables that may serve as indicators of *Illex* habitat condition or areas of increased primary productivity. These indicators are of interest due to their implications for identifying potential areas that may support *Illex* aggregation and transport, which can provide a better understanding of their availability to the fishery.

#### 4.1 | Indicators of habitat condition

Bottom temperature and RFI may be useful indicators for habitat conditions, whereas the remaining covariates, ring orientation, salinity at depth, and chlorophyll frontal dynamics are potential indicators of areas of high primary productivity. Results from GAMs identified low mean bottom temperatures as a strong predictor of CPUE, which is consistent with results from surveys done by Hendrickson (2004), where juveniles were primarily found in deeper waters (140–260 m) and associated with bottom temperatures at the low end of the sampled range (9.9–13.5°C). Existing hypotheses around the relationship between *Illex* occurrence and cooler bottom temperatures have been attributed to the selection of cooler habitat conditions as a means to manage metabolic demands as well as the use of depth to avoid predation (Benoit-Bird & Moline, 2021; Perez & O'Dor, 1998). The relationship of high *Illex* CPUE with low bottom temperatures strongly suggests that the *Illex* available to the US fishery are primarily associated with the cooler, shelf water (onshore-side) of the Shelfbreak Front. An important caveat to this interpretation is that bottom temperatures on the shelf are highly dependent on local processes (e.g., circulation and intrusions) and variable in space and time (Chen et al., 2021), and we currently lack offshore (Slope Sea) data to test the full extent of the bottom temperature range *Illex* experiences. Therefore, more research is needed to better understand the importance of bottom temperature on the juvenile and adult life history stages of *Illex*.

The lagged RFI, a measure of ring occupancy in the Slope Sea, may serve as an additional indicator of habitat condition for larval/pre-recruit stages. Examining ring footprints in the Slope Sea at 6- and 3-month lag times was an effort to (i) understand water conditions in areas previously identified as important for larval stages of the *Illex* (Bakun & Csirke, 1998; Dawe et al., 2007) and (ii) gain insight into rings as potential transport and retention mechanisms. Recent statolith-based age analyses indicated year-round spawning with two dominant cohorts specific to the *Illex* fishery, a winter cohort hatching between January and March and a summer cohort with hatch dates during the months of May through July (Hendrickson, 2004). As specific hatch times vary inter-annually, having an indication of the total area of the Slope Sea occupied by WCRs during the winter hatch months (January–March) could provide a powerful tool for understanding the variability of the habitat conditions (salinity, temperature, and productivity) to which newly hatched *Illex* are exposed and the potential for their physical transport to the shelf break. Therefore, the significant relationship that emerged between catch and a lagged RFI in Slope Sea Zones 1–3 (higher catch at RFI > .3 in Zones 2 and 3 lagged by 6 months and Zone 1 lagged by 3 months; see Figure 7g,h,i) is an important result that merits further investigation as it may have implications as a pre-season indicator. For instance, a larger RFI in Zone 2 equates to a significant presence of anticyclonic rings traveling in a southwesterly direction (towards the shelf break) 6 months ahead of the summer fishery. It is plausible that the increased amount of area occupied by rings in the Slope Sea in the winter months would equate to higher potential for paralarvae to be

transported to the shelf from their origination along the north wall of the GS (Hare et al., 2002; Hatanaka et al., 1985). Furthermore, we would expect the RFI in Zone 1 to have influences on the fishery at shorter lag times (e.g., 3 months), as the distance necessary to transport organisms from the north wall of the GS to the shelf break is smaller (Figures 3 and 7h). Following this logic, the effects of WCRs further East of Zone 3 (<60°W) were not included in the final analysis, as they are less likely to migrate to the Mid-Atlantic Bight region of the continental shelf (e.g., Zones 1 and 2 vs. Zone 4; Silva et al., 2020). We suspect the presence of rings beyond Zone 3 are more likely to act as a retention mechanism (as opposed to a transport mechanism) with the potential of retaining paralarvae and juveniles in the Slope Sea, thus rendering that portion of the population unavailable to the US fishery. Thus, the geographical location of a WCR is a key aspect to consider (in addition to quantity and time of occupancy) in effort to identify which rings may be relevant indicators of *Illex* availability.

The insights gleaned from examining trends in habitat condition during winter hatching seasons (prior to start of the late spring, early summer fishing season) would benefit from targeted larval surveys along the north wall of the GS throughout Zones 1–3 during the proposed hatching months (Hendrickson, 2004). Quantifying the presence and timing of these mesoscale eddies in areas occupied by *Illex* during early life history stages prior to the start of the fishing season can improve our ability to forward-project the potential availability of mature squid to the summer and fall fishery.

#### 4.2 | Indicators of areas of high primary productivity

The remaining covariates can be summed up as indicators of areas of high primary productivity. Hot spots of primary productivity are of interest for this mid-level consumer, as they can serve as an indirect proxy for food availability. The lower variability and higher catch associated with the eastern orientation of a WCR to a fishing point are in alignment with our hypotheses that *Illex* abundance is likely to be more concentrated on the eastern edge of a WCR than the western edge. Specifically, Forsyth et al. (2022) found that as a WCR impinges on the shelf, an interaction occurs between the shelf streamer, created on its eastern edge, and the MAB Shelfbreak Jet that results in significant increases in upwelling (by a factor of 10) and enhanced primary productivity (Cenedese et al., 2013; Forsyth et al., 2020; Gawarkiewicz et al., 2001). Therefore, ring orientation could serve as a potential mechanism supporting the aggregation and feeding of juveniles and adults. While the trend is clear, the lack of significant difference in CPUE associated with the eastern and western side of a WCR in this analysis is driven by the large variation in catch on the western side of rings. This is likely due to the complexity of ring/shelf dynamics. For instance, in a given week, there may be multiple rings impinging on the shelf simultaneously, and depending on their locations in space and time, this can result in very complex cross-shelf exchange processes. To this end, while ring orientation was calculated

for the closest ring to a given fishing point, there can be instances where a fishing location is in between two rings.

The strong significant relationship between high catch and subsurface salinity greater than 35.6 (at 222 m depth, Figure 7f) indicates a meaningful relationship between the presence of GS water and *Illex* squid. Surface (and near-surface) salinity measurements are highly variable due to the mixing of surface waters, whereas a high salinity signal at depth can indicate the presence of a WCR. Additionally, the 200 m isobath is roughly the mean position of the MAB Shelfbreak Jet (Forsyth et al., 2020). The interaction of the Shelfbreak Jet and the highly saline ring water has the potential to support high levels of primary productivity via upwelling, which can reach the location of the 26.0 kg m<sup>-3</sup> isopycnal (Forsyth et al., 2020; Oliver et al., 2021). Therefore, due to the potential for cross-shelf exchange processes that can occur when GS water interacts with the shelf, subsurface salinity (measured here at 222 m depth) is an indirect indicator of primary productivity. This location is also coincident with the near-bottom preference of *Illex* squid. The initial peak in catch for salinities between 35.2 and 35.3 are likely signals of older rings that have mixed with surrounding slope water, characterized by smaller diameters and less vertical extent than rings with higher salinities of 35.7–35.8 (Gawarkiewicz et al., 2001; Silva et al., 2020).

The nonlinear trend relating catch rates to proportions of the shelfbreak region identified as chlorophyll-*a* fronts is complex. Part of this complexity stems from the fact that during the summer stratified season, nutrients are often not mixed to the surface layers, and the subsurface chlorophyll maximum is typically below the detection depth of ocean color remote sensors. Even so, we see higher catch associated with higher proportions of the Shelfbreak region classified as chlorophyll fronts, suggesting that when detectable, chlorophyll fronts may serve as a productivity hotspot indicator, with biological implications for benthopelagic species such as *Illex* squid. The highest amount of variation in SST occurs at the Shelfbreak Front region (Linder & Gawarkiewicz, 1998), which is also the location of the majority of the fishing effort. The ecological interpretation of this trend is less clear as the variability in SST may simply be acting as an indicator for capturing heterogeneity in position of the Shelfbreak Front. In addition, subsurface influences, including bathymetric features (such as high slope), could be affecting either (or both) the location of squid aggregations or the ability to harvest them. This relationship may serve as a useful indicator of changes in the water composition, as increased standard deviations in SST are likely related to instances of variability in the mean position of the Shelfbreak Front or slope water intrusions onto the shelf.

## 5 | SUMMARY AND CONCLUSION

By combining knowledge about the dynamics of the physical oceanography in the region with the current ecological and observational understanding of this species, we were able to construct a model that represents a reasonable hypothesis about how this system works. In

sum, habitat conditions indicated by bottom temperatures and the timing, size, and location of WCRs as well as indicators of areas of high primary productivity, including subsurface salinity, chlorophyll fronts, and the variability of SST explained over 50% of the variation in CPUE for the *Illex* fishery over the past 10 years. Specifically, (i) cooler bottom temperatures, (ii) higher instances of RFI in the winter and early spring months (ahead of the summer fishery), and (iii) physical processes that promote upwelling (e.g., frontal dynamics and interactions between WCRs and subsurface features) are associated with greater CPUE.

While these results are correlative in nature, they have strong implications for understanding the mechanistic drivers of *Illex* distribution throughout the fishery in space and time. More research is needed to identify and verify these potential drivers in order to move towards in-season management and pre-season forecasting. Future research initiatives would benefit from increased *Illex* sampling efforts throughout the Slope Sea across multiple life history stages (e.g., larval, juvenile, and adult) and identification of *Illex* spawning locations, as well as cooperative research aboard commercial fishing vessels to quantify *Illex* within and around WCRs during the fishing season. Furthermore, while our model corroborates and extends hypotheses that bottom-up forces (i.e., oceanographic processes) are driving the inter-annual variability in the availability of *Illex* to the US fishery (Table 2, 56% of variance explained), more research is needed to examine the role of top-down processes. The inter-annual variability of fishing location is the product of a nuanced combination of socioeconomic and oceanographic factors. To capture the extent of the complexity of the variability in this fishery, future work needs to disentangle the complex effect of fishing behavior on CPUE. Ongoing collaborations between industry partners, harvesters, and scientists has provided great insight into this complexity, highlighting the importance of global market preferences and fuel prices in combination with changing fishing fleets and processor infrastructure (Lowman, Jones, & Mercer, 2021; Mercer et al., 2022). This is particularly relevant for this species, as was detailed by Mercer et al. (2022), who suggest that due to their sensitivities to fleet and marketing dynamics, landing trends for *Illex* have the potential to become decoupled from biological indicators. Deciphering whether particular instances of high catch reflect fishing behavior (e.g., gear restrictions, vessel capacities, etc.) or true *Illex* aggregations is an important next step.

Increased understanding of the role of environmental conditions and the mechanistic oceanographic underpinnings driving the ingress and egress events of *Illex* is an invaluable part of its stock assessment and management. In particular, for data poor species, research efforts such as this, linking oceanographic conditions to stock conditions, have the potential to inform management policies by reducing uncertainties related to availability and productivity. Thus, this study details a useful framework for the development of fine-scale oceanographic indicators that can be applied to other commercially important species. The US *Illex* fishery serves as an example of the insights and understanding of a data-limited stock that is achievable through open collaboration and innovation across sectors.

## AUTHOR CONTRIBUTIONS

SS, KH, AM, SG, and JM conceived the study. BL, KH, AS, SS, DH, BG, and AJ collected and curated the data. SS, KH, AS, AG, and GG derived oceanographic metrics. All authors contributed to the development of the conceptual model. SS conducted the statistical analyses with substantial input from DH, BG, JM, SG, KH, and AM. SS wrote the original draft. All authors interpreted the results, contributed substantial edits to the manuscript, and approved the submitted version.

## ACKNOWLEDGMENTS

We gratefully acknowledge Jimmy Ruhle (F/V Darana R), Lisa Hendrickson (NEFSC), Paula Fratantoni (NEFSC), Paul Rago (MAFMC), and Steve Lorenz (UMASSD-SMAST) for all their valuable contributions to this work.


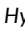

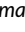
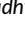
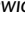
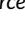
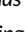

## CONFLICT OF INTEREST

The authors declare that the research was conducted in the absence of any commercial or financial relationships that could be construed as a potential conflict of interest.

## DATA AVAILABILITY STATEMENT

Publicly available satellite and oceanographic datasets were analyzed in this study. The Multiscale Ultra-high Resolution (MUR; v4.1) sea surface temperature satellite data can be sourced online (at [https://podaac.jpl.nasa.gov/dataset/MUR-JPL-L4-GLOB-v4.1?ids=GridSpatialResolution:ProcessingLevel&values=0.01:\\*4\\*&search=GHRSSST](https://podaac.jpl.nasa.gov/dataset/MUR-JPL-L4-GLOB-v4.1?ids=GridSpatialResolution:ProcessingLevel&values=0.01:*4*&search=GHRSSST)), and the Ocean Color–Climate Change Initiative (OC-CCI; v5.0) chlorophyll data are available from the European Space Agency website (<https://climate.esa.int/en/projects/ocean-colour/>). Chlorophyll fronts were derived using the Belkin and O'Reilly front detection model (Belkin & O'Reilly, 2009). The Global Ocean Reanalysis Model (GLORYS 12v1) data are available online (via [https://data.marine.copernicus.eu/product/GLOBAL\\_ANALYSIS\\_FORECAST\\_PHY\\_001\\_024/description](https://data.marine.copernicus.eu/product/GLOBAL_ANALYSIS_FORECAST_PHY_001_024/description)). The Warm Core Ring trajectory information (2011–2020) is available online (at <https://doi.org/10.5281/zenodo.6436380>). Study Fleet and Observer fishery dependent data are confidential, according to NAO 216-100, but can be made available in aggregated form upon request. For Observer data, please contact Gina Shield ([gina.shield@noaa.gov](mailto:gina.shield@noaa.gov)). For Study Fleet data, please contact Anna Mercer ([anna.mercer@noaa.gov](mailto:anna.mercer@noaa.gov)).

## ORCID

Sarah L. Salois  <https://orcid.org/0000-0002-0756-0778>  
 Kimberly J. W. Hyde  <https://orcid.org/0000-0002-1564-5499>  
 Adrienne Silver  <https://orcid.org/0000-0002-6078-0577>  
 Brooke A. Lowman  <https://orcid.org/0000-0002-9301-799X>  
 Avijit Gangopadhyay  <https://orcid.org/0000-0002-7412-7325>  
 Glen Gawarkiewicz  <https://orcid.org/0000-0001-9629-3300>  
 Anna J. M. Mercer  <https://orcid.org/0000-0002-8158-6570>  
 Sarah K. Gaichas  <https://orcid.org/0000-0002-5788-3073>  
 Daniel J. Hocking  <https://orcid.org/0000-0003-1889-9184>

## REFERENCES

- Anderson, D., & Burnham, K. (2004). *Model selection and multi-model inference* (Second ed., Vol. 63) (p. 10). Springer-Verlag.
- Andres, M. (2016). On the recent destabilization of the Gulf Stream path downstream of Cape Hatteras. *Geophysical Research Letters*, 43, 9836–9842. <https://doi.org/10.1002/2016GL069966>
- Arkipkin, A. I., Rodhouse, P. G. K., Pierce, G. J., Sauer, W., Sakai, M., Allcock, L., Arguelles, J., Bower, J. R., Castillo, G., Ceriola, L., Chen, C.-S., Chen, X., Diaz-Santana, M., Downey, N., González, A. F., Granados Amores, J., Green, C. P., Guerra, A., Hendrickson, L. C., ... Zeidberg, L. D. (2015). World squid fisheries. *Reviews in Fisheries Science & Aquaculture*, 23, 92–252. <https://doi.org/10.1080/23308249.2015.1026226>
- Bakun, A., & Csirke, J. (1998). Environmental processes and recruitment variability. pp. 105–124 FAO Fisheries Technical Paper.
- Belkin, I. M., & O'Reilly, J. E. (2009). An algorithm for oceanic front detection in chlorophyll and SST satellite imagery. *Journal of Marine Systems*, 78, 319–326. <https://doi.org/10.1016/j.jmarsys.2008.11.018>
- Benoit-Bird, K. J., & Moline, M. A. (2021). Vertical migration timing illuminates the importance of visual and nonvisual predation pressure in the mesopelagic zone. *Limnology and Oceanography*, 66, 3010–3019. <https://doi.org/10.1002/lno.11855>
- Bisagni, J. J. (1983). Lagrangian current measurements within the eastern margin of a warm-core gulf stream ring. *Journal of Physical Oceanography*, 13, 709–715. [https://doi.org/10.1175/1520-0485\(1983\)013<0709:LCMWTE>2.0.CO;2](https://doi.org/10.1175/1520-0485(1983)013<0709:LCMWTE>2.0.CO;2)
- Bisagni, J. J., Nichols, O. C., & Pettipas, R. (2019). Interannual variability of Gulf Stream warm-core ring interactions with the outer continental shelf and potential broad scale relationships with longfin squid (*Doryteuthis pealeii*) relative abundance, 1981–2004. *ICES Journal of Marine Science*, 76, 1257–1270.
- Bost, C. A., Cotté, C., Bailleul, F., Cherel, Y., Charrassin, J. B., Guinet, C., Ainley, D. G., & Weimerskirch, H. (2009). The importance of oceanographic fronts to marine birds and mammals of the southern oceans. *Journal of Marine Systems*, 78, 363–376. <https://doi.org/10.1016/j.jmarsys.2008.11.022>
- Brodziak, J., & Walsh, W. A. (2013). Model selection and multimodel inference for standardizing catch rates of bycatch species: A case study of oceanic whitetip shark in the Hawaii-based longline fishery. *Canadian Journal of Fisheries and Aquatic Sciences*, 70, 1723–1740. <https://doi.org/10.1139/cjfas-2013-0111>
- Cenedese, C., Todd, R. E., Gawarkiewicz, G. G., Owens, W. B., & Shcherbina, A. Y. (2013). Offshore transport of shelf waters through interaction of vortices with a shelfbreak current. *Journal of Physical Oceanography*, 43, 905–919. <https://doi.org/10.1175/JPO-D-12-0150.1>
- Chen, K., Gawarkiewicz, G. G., Lentz, S. J., & Bane, J. M. (2013). Diagnosing the warming of the Northeastern U.S. Coastal Ocean in 2012: A linkage between the atmospheric jet stream variability and ocean response. *Journal of Geophysical Research, Oceans*, 119, 218–227.
- Chen, Z., Kwon, Y., Chen, K., Fratantoni, P., Gawarkiewicz, G., & Joyce, T. M. (2020). Long-term SST variability on the Northwest Atlantic continental shelf and slope. *Geophysical Research Letters*, 47, e2019GL085455. <https://doi.org/10.1029/2019GL085455>
- Chen, Z., Kwon, Y.-O., Chen, K., Fratantoni, P., Gawarkiewicz, G., Joyce, T. M., Miller, T. J., Nye, J. A., Saba, V. S., & Stock, B. C. (2021). Seasonal prediction of bottom temperature on the northeast U.S. continental shelf. *Journal of Geophysical Research, Oceans*, 126, e2021JC017187.
- Chin, T. M., Vazquez-Cuervo, J., & Armstrong, E. M. (2017). A multi-scale high-resolution analysis of global sea surface temperature. *Remote Sensing of Environment*, 200, 154–169. <https://doi.org/10.1016/j.rse.2017.07.029>

- Clay, P. M., Howard, J., Busch, D. S., Colburn, L. L., Himes-Cornell, A., Rumrill, S. S., Zador, S. G., & Griffis, R. B. (2020). Ocean and coastal indicators: Understanding and coping with climate change at the land-sea interface. *Climatic Change*, 163, 1773–1793. <https://doi.org/10.1007/s10584-020-02940-x>
- CMEMS (2018) GLORYS12V1 - Global Ocean Physical Reanalysis Product E.U. Copernicus Marine Service Information. <https://doi.org/10.48670/moi-00021>
- Dawe, E. G., & Beck, P. C. (1997). Population structure, growth, and sexual maturation of short-finned squid (*Illex illecebrosus*) at Newfoundland. *Canadian Journal of Fisheries and Aquatic Sciences*, 54, 137–146. <https://doi.org/10.1139/f96-263>
- Dawe, E. G., Hendrickson, L. C., Colbourne, E. B., Drinkwater, K. F., & Showell, M. A. (2007). Ocean climate effects on the relative abundance of short-finned (*Illex illecebrosus*) and long-finned (*Loligo pealeii*) squid in the northwest Atlantic Ocean. *Fisheries Oceanography*, 16, 303–316. <https://doi.org/10.1111/j.1365-2419.2007.00431.x>
- DePiper, G. S., Gaichas, S. K., Lucey, S. M., Pinto da Silva, P., Anderson, M. R., Breeze, H., Bundy, A., Clay, P. M., Fay, G., Gamble, R. J., Gregory, R. S., Fratantoni, P. S., Johnson, C. L., Koen-Alonso, M., Kleisner, K. M., Olson, J., Perretti, C. T., Pepin, P., Phelan, F., ... Wildermuth, R. P. (2017). Operationalizing integrated ecosystem assessments within a multidisciplinary team: Lessons learned from a worked example. *ICES Journal of Marine Science*, 74, 2076–2086. <https://doi.org/10.1093/icesjms/fsx038>
- Drinkwater, K., Lochman, S., Taggart, C., Thompson, K., & Frank, K. (2000). Entrainment of redfish (*Sebastes* spp.) larvae off the Scotian Shelf. *ICES Journal of Marine Science*, 57, 372–382. <https://doi.org/10.1006/jmsc.1999.0602>
- du Pontavice, H., Miller, T. J., Stock, B. C., Chen, Z., & Saba, V. S. (2022). Ocean model-based covariates improve a marine fish stock assessment when observations are limited. *ICES Journal of Marine Science*, 79, 1259–1273. <https://doi.org/10.1093/icesjms/fsac050>
- Fernandez, E., & Lellouche, J. M. (2018). Product user manual for the global ocean physical reanalysis product GLORYS12V1. *Copernicus Product User Manual*, 4, 1–15.
- Forsyth, J., Andres, M., & Gawarkiewicz, G. (2020). Shelfbreak jet structure and variability off New Jersey using ship of opportunity data from the CMV Oleander. *Journal of Geophysical Research, Oceans*, 125, e2020JC016455. <https://doi.org/10.1029/2020JC016455>
- Forsyth, J., Gawarkiewicz, G., & Andres, M. (2022). The impact of warm Core rings on Middle Atlantic Bight shelf temperature and shelf break velocity. *Journal of Geophysical Research, Oceans*, 127. <https://doi.org/10.1029/2021JC017759>
- Forsyth, J. S. T., Andres, M., & Gawarkiewicz, G. G. (2015). Recent accelerated warming of the continental shelf off New Jersey: Observations from the CMV Oleander expendable bathythermograph line. *Journal of Geophysical Research, Oceans*, 120, 2370–2384. <https://doi.org/10.1002/2014JC010516>
- Fu, C., Gaichas, S., Link, J., Bundy, A., Boldt, J., Cook, A., Gamble, R., Rong Utne, K., Liu, H., & Friedland, K. (2012). Relative importance of fisheries, trophodynamic and environmental drivers in a series of marine ecosystems. *Marine Ecology Progress Series*, 459, 169–184. <https://doi.org/10.3354/meps09805>
- Gangopadhyay, A., Gawarkiewicz, G., Silva, E. N. S., Monim, M., & Clark, J. (2019). An observed regime shift in the formation of warm core rings from the Gulf Stream. *Scientific Reports*, 9, 12319. <https://doi.org/10.1038/s41598-019-48661-9>
- Gangopadhyay, A., Gawarkiewicz, G., Silva, E. N. S., Silver, A. M., Monim, M., & Clark, J. (2020). A census of the warm-core rings of the Gulf Stream: 1980–2017. *Journal of Geophysical Research, Oceans*, 125, e2019JC016033. <https://doi.org/10.1029/2019JC016033>
- Gawarkiewicz, G., Bahr, F., Beardsley, R. C., & Brink, K. H. (2001). Interaction of a slope eddy with the shelfbreak front in the Middle Atlantic Bight. *Journal of Physical Oceanography*, 31, 14–2796. [https://doi.org/10.1175/1520-0485\(2001\)031<2783:IOASEW>2.0.CO;2](https://doi.org/10.1175/1520-0485(2001)031<2783:IOASEW>2.0.CO;2)
- Gawarkiewicz, G., Chen, K., Forsyth, J., Bahr, F., Mercer, A. M., Ellertson, A., Fratantoni, P., Seim, H., Haines, S., & Han, L. (2019). Characteristics of an advective marine heatwave in the Middle Atlantic Bight in early 2017. *Frontiers in Marine Science*, 6, 712. <https://doi.org/10.3389/fmars.2019.00712>
- Gawarkiewicz, G., Fratantoni, P., Bahr, F., & Ellertson, A. (2022). Increasing frequency of mid-depth salinity maximum intrusions in the Middle Atlantic Bight. *Journal of Geophysical Research, Oceans*, 127, e2021JC018233. <https://doi.org/10.1029/2021JC018233>
- Gawarkiewicz, G., Todd, R., Zhang, W., Partida, J., Gangopadhyay, A., Monim, M.-U.-H., Fratantoni, P., Malek Mercer, A., & Dent, M. (2018). The changing nature of shelf-break exchange revealed by the OOI Pioneer Array. *Oceanography*, 31, 60–70. <https://doi.org/10.5670/oceanog.2018.110>
- Gonçalves Neto, A., Langan, J. A., & Palter, J. B. (2021). Changes in the Gulf Stream preceded rapid warming of the Northwest Atlantic Shelf. *Communications Earth & Environment*, 2, 74. <https://doi.org/10.1038/s43247-021-00143-5>
- Großelindemann, H., Ryan, S., Ummenhofer, C. C., Martin, T., & Biastoch, A. (2022). Marine heatwaves and their depth structures on the northeast U.S. continental shelf. *Frontiers in Climate*, 4, 857937. <https://doi.org/10.3389/fclim.2022.857937>
- Haltuch, M. A., Tolimieri, N., Lee, Q., & Jacox, M. G. (2020). Oceanographic drivers of petrale sole recruitment in the California Current Ecosystem. *Fisheries Oceanography*, 29, 122–136. <https://doi.org/10.1111/fog.12459>
- Harden, B. E., Gawarkiewicz, G. G., & Infante, M. (2020). Trends in physical properties at the southern New England shelf break. *Journal of Geophysical Research, Oceans*, 125, e2019JC015784. <https://doi.org/10.1029/2019JC015784>
- Hare, J. A., Churchill, J. H., Cowen, R. K., Berger, T. J., Cornillon, P. C., Dragos, P., Glenn, S. M., Govoni, J. J., & Lee, T. N. (2002). Routes and rates of larval fish transport from the southeast to the northeast United States continental shelf. *Limnology and Oceanography*, 47, 1774–1789. <https://doi.org/10.4319/lo.2002.47.6.1774>
- Harley, S. J., Ransom A. M., & Alistair, D. (2001). Is catch-per-unit-effort proportional to abundance. *Canadian Journal of Fisheries and Aquatic Sciences*, 58(9), 1760–1772.
- Hatanaka, H., Lange, A. M. T., Hole, W., & Amaratunga, T. (1985). Geographical and vertical distribution of short-finned squid (*Illex illecebrosus*) larvae in the Northwest Atlantic. *NAFO Science Council Studies*, 9, 93–99.
- Hendrickson, L. C. (2004). Population biology of northern shortfin squid (*Illex illecebrosus*) in the Northwest Atlantic Ocean and initial documentation of a spawning area. *ICES Journal of Marine Science*, 61, 252–266. <https://doi.org/10.1016/j.icesjms.2003.10.010>
- Hendrickson, L. C., & Holmes, E. M. (2004). Northern Shortfin Squid, *Illex illecebrosus*, Life History and Habitat Characteristics. NOAA Technical Memorandum NMFS-NE-191:46.
- Hendrickson, L. C., & Showell, M. A. (2019). Assessment of Northern Shortfin Squid (*Illex illecebrosus*) in Subareas 3+4. NAFO SCR Doc. 19/042, Serial No. N6973. 38 p.
- Hoarfrost, A., Balmonte, J. P., Ghobrial, S., Ziervogel, K., Bane, J., Gawarkiewicz, G., & Arnosti, C. (2019). Gulf stream ring water intrusion on the mid-Atlantic bight continental shelf break affects microbially driven carbon cycling. *Frontiers in Marine Science*, 6, 394. <https://doi.org/10.3389/fmars.2019.00394>
- Hobday, A. J., Alexander, L. V., Perkins, S. E., Smale, D. A., Straub, S. C., Oliver, E. C. J., Benthuyens, J. A., Burrows, M. T., Donat, M. G., Feng, M., Holbrook, N. J., Moore, P. J., Scannell, H. A., Sen Gupta, A., & Wernberg, T. (2016). A hierarchical approach to defining marine heatwaves. *Progress in Oceanography*, 141, 227–238. <https://doi.org/10.1016/j.pocean.2015.12.014>



- Houghton, R. W., & Visbeck, M. (1998). Upwelling and convergence in the Middle Atlantic Bight Shelfbreak Front. *Geophysical Research Letters*, 25, 2765–2768. <https://doi.org/10.1029/98GL02105>
- Jones, A. W., Burchard, K. A., Mercer, A. M., Hoey, J. J., Morin, M. D., Gianesin, G. L., Wilson, J. A., Alexander, C. R., Lowman, B. A., Duarte, D. G., Goethel, D., Ford, J., Ruhle, J., Sykes, R., & Sawyer, T. (2022). Learning from the study fleet: Maintenance of a large-scale reference fleet for northeast U.S. fisheries. *Frontiers in Marine Science*, 9. <https://doi.org/10.3389/fmars.2022.869560>
- Jones, A. W., Lowman, B. L., Manderson, J. M., & Mercer, A. (2020). An investigation of fine-scale CPUE for northern shortfin squid (*Illex illecebrosus*) using NEFSC Study Fleet data. Working Paper for the MAFMC Illex Working Group and Science and Statistical Committee.
- Joyce, T. M. (1984). Velocity and hydrographic structure of a gulf stream warm-core ring. *Journal of Physical Oceanography*, 14, 936–947. [https://doi.org/10.1175/1520-0485\(1984\)014<0936:VAHSOA>2.0.CO;2](https://doi.org/10.1175/1520-0485(1984)014<0936:VAHSOA>2.0.CO;2)
- Joyce, T. M. (1985). Gulf stream warm-core ring collection: An introduction. *Journal of Geophysical Research*, Oceans, 90, 8801–8802. <https://doi.org/10.1029/JC090iC05p08801>
- Lellouche, J. M., Bourdalle-Badie, R., Greiner, E., Garric, G., Melet, A., Bricaud, C., Legalloudec, O., Hamon, M., Candela, T., Regnier, C., & Drevillon, M. (2021). The Copernicus global 1/12° oceanic and sea ice reanalysis: EGU21-14961.
- Levin, P. S., Breslow, S. J., Harvey, C. J., Norman, K. C., Poe, M. R., Williams, G. D., & Plummer, M. L. (2016). Conceptualization of social-ecological systems of the California Current: An examination of interdisciplinary science supporting ecosystem-based management. *Coastal Management*, 44, 397–408. <https://doi.org/10.1080/08920753.2016.1208036>
- Linder, C. A., & Gawarkiewicz, G. (1998). A climatology of the shelfbreak front in the Middle Atlantic Bight. *Journal of Geophysical Research*, Oceans, 103, 18405–18423. <https://doi.org/10.1029/98JC01438>
- Lowman, B. A., Jones, A. W., & Mercer, A. (2021). Northern shortfin squid landings per unit effort. Working paper for the MAFMC Illex Working Group and Science and Statistical Committee.
- Lowman, B. A., Jones, A. W., Pessutti, J. P., Mercer, A. M., Manderson, J. P., & Galuardi, B. (2021). Northern shortfin squid (*Illex illecebrosus*) fishery footprint on the northeast US continental shelf. *Frontiers in Marine Science*, 8, 631657. <https://doi.org/10.3389/fmars.2021.631657>
- Mercer, A. J., Manderson, J. P., Rago, P. J., Lowman, B., Pessutti, J., Wilson, J., Gianesin, G., Alexander, C., Almeida, K., Amory, M., Clarke, R., Goodwin, G., Kaelin, J., Lapp, M., Mitchell, B., O'Neill, G., Ruhle, J., Reichle, W., Reid, E., ... Jordan, J. (2022). Technical and economic aspects of northern shortfin squid (*Illex illecebrosus*) processing and marketing essential for interpreting of fishing effort and catch as indicators of population trend and condition. Working Paper for the 2021 Illex Research Track Stock Assessment. Accessed at [https://apps-nefsc.fisheries.noaa.gov/saw/sasi/sasi\\_report\\_options.php](https://apps-nefsc.fisheries.noaa.gov/saw/sasi/sasi_report_options.php)
- Miller, P. (2009). Composite front maps for improved visibility of dynamic sea-surface features on cloudy SeaWiFS and AVHRR data. *Journal of Marine Systems*, 78, 327–336. <https://doi.org/10.1016/j.jmarsys.2008.11.019>
- Miller, P. I., & Christodoulou, S. (2014). Frequent locations of oceanic fronts as an indicator of pelagic diversity: Application to marine protected areas and renewables. *Marine Policy*, 45, 318–329. <https://doi.org/10.1016/j.marpol.2013.09.009>
- Miller, P. I., Scales, K. L., Ingram, S. N., Southall, E. J., & Sims, D. W. (2015). Basking sharks and oceanographic fronts: Quantifying associations in the north-east Atlantic. *Functional Ecology*, 29, 1099–1109. <https://doi.org/10.1111/1365-2435.12423>
- Morgan, C. W., & Bishop, J. M. (1977). An example of gulf stream eddy-induced water exchange in the Mid-Atlantic Bight. *Journal of Physical Oceanography*, 7, 472–479. [https://doi.org/10.1175/1520-0485\(1977\)007<0472:AEOGSE>2.0.CO;2](https://doi.org/10.1175/1520-0485(1977)007<0472:AEOGSE>2.0.CO;2)
- Myers, R. A., & Drinkwater, K. (1989). The influence of Gulf Stream warm core rings on recruitment of fish in the northwest Atlantic. *Journal of Marine Research*, 47, 635–656. <https://doi.org/10.1357/002224089785076208>
- New, A. L., Smeed, D. A., Czaja, A., Blaker, A. T., Mecking, J. V., Mathews, J. P., & Sanchez-Franks, A. (2021). Labrador slope water connects the subarctic with the Gulf Stream. *Environmental Research Letters*, 16, 084019. <https://doi.org/10.1088/1748-9326/ac1293>
- Northeast Fisheries Science Center [NEFSC] (2006). 42nd Northeast Regional Stock Assessment Workshop (42nd SAW) Stock Assessment Report Part A: Silver Hake, Mackerel, & Northern Shortfin Squid: Northeast Fish. Sci. Cent. Ref. Doc. 06–09a. (Woods Hole, MA: Northeast Fisheries Science Center).
- Oliver, H., Zhang, W. G., Smith, W. O., Alatalo, P., Chappell, P. D., Hirzel, A. J., Selden, C. R., Sosik, H. M., Stanley, R. H. R., Zhu, Y., & McGillicuddy, D. J. (2021). Diatom hotspots driven by western boundary current instability. *Geophysical Research Letters*, 48, e2020GL091943. <https://doi.org/10.1029/2020GL091943>
- Palacios-Abrantes, J., Reygondeau, G., Wabnitz, C. C. C., & Cheung, W. W. L. (2020). The transboundary nature of the world's exploited marine species. *Scientific Reports*, 10, 17668. <https://doi.org/10.1038/s41598-020-74644-2>
- Palmer, M. C., Hersey, P., Marotta, H., Shield, G. R., & Cierpich, S. B. (2016). The design and performance of an automated observer deployment system for the Northeastern United States groundfish fishery. *Fisheries Research*, 179, 33–46. <https://doi.org/10.1016/j.fishres.2016.02.004>
- Pedersen, E. J., Miller, D. L., Simpson, G. L., & Ross, N. (2019). Hierarchical generalized additive models in ecology: An introduction with mgcv. *PeerJ*, 7, e6876. <https://doi.org/10.7717/peerj.6876>
- Perez, E., Ryan, S., Andres, M., Gawarkiewicz, G., Ummenhofer, C. C., Bane, J., & Haines, S. (2021). Understanding physical drivers of the 2015/16 marine heatwaves in the Northwest Atlantic. *Scientific Reports*, 11, 17623. <https://doi.org/10.1038/s41598-021-97012-0>
- Perez, J. A. A., & O'Dor, R. K. (1998). The impact of environmental gradients on the early life inshore migration of the short-finned squid *Illex illecebrosus*. *South African Journal of Marine Science*, 20, 293–303. <https://doi.org/10.2989/025776198784126359>
- Pershing, A. J., Alexander, M. A., Hernandez, C. M., Kerr, L. A., le Bris, A., Mills, K. E., Nye, J. A., Record, N. R., Scannell, H. A., Scott, J. D., Sherwood, G. D., & Thomas, A. C. (2015). Slow adaptation in the face of rapid warming leads to collapse of the Gulf of Maine cod fishery. *Science*, 350, 809–812. <https://doi.org/10.1126/science.aac9819>
- Polovina, J. J., & Howell, E. A. (2005). Ecosystem indicators derived from satellite remotely sensed oceanographic data for the North Pacific. *ICES Journal of Marine Science*, 62, 319–327. <https://doi.org/10.1016/j.icesjms.2004.07.031>
- QGIS Development Team. (2016). QGIS Geographic Information System.
- R Core Team. (2021). R: A language and environment for statistical computing. R Foundation for Statistical Computing. Vienna, Austria. <https://www.R-project.org/>
- Ryan, J. P., Yoder, J. A., Barth, J. A., & Cornillon, P. C. (1999). Chlorophyll enhancement and mixing associated with meanders of the shelf break front in the Mid-Atlantic Bight. *Journal of Geophysical Research*, Oceans, 104, 23479–23493. <https://doi.org/10.1029/1999JC900174>
- Saba, V. S., Hyde, K. J. W., Rebuck, N. D., Friedland, K. D., Hare, J. A., Kahru, M., & Fogarty, M. J. (2015). Physical associations to spring phytoplankton biomass interannual variability in the U.S. Northeast Continental Shelf: NW Atlantic chlorophyll variability. *Journal of Geophysical Research: Biogeosciences*, 120, 205–220. <https://doi.org/10.1002/2014JG002770>
- Sathyendranath, S., Brewin, R. J. W., Brockmann, C., Brotas, V., Calton, B., Chuprin, A., Cipollini, P., Couto, A. B., Dingle, J., Doerffer, R., Donlon, C., Dowell, M., Farman, A., Grant, M., Groom, S., Horseman, A., Jackson, T., Krasemann, H., Lavender, S., ... Platt, T.

- (2019). An ocean-colour time series for use in climate studies: The experience of the ocean-colour climate change initiative (OC-CCI). *Sensors*, 19, 4285. <https://doi.org/10.3390/s19194285>
- Sathyendranath, S., Jackson, T., Brockmann, C., Brotas, V., Calton, B., Chuprin, A., Clements, O., Cipollini, P., Danne, O., Dingle, J., Donlon, C., Grant, M., Groom, S., Krasemann, H., Lavender, S., Mazeran, C., Mélin, F., Müller, D., Steinmetz, F., ... Platt, T. (2021). ESA Ocean Colour Climate Change Initiative (Ocean\_Colour\_cci): Version 5.0 Data. NERC EDS Centre for Environmental Data Analysis. <https://doi.org/10.5285/1dbe7a109c0244aad713e078fd3059a>
- Seidov, D., Mishonov, A., & Parsons, R. (2021). Recent warming and decadal variability of Gulf of Maine and slope water. *Limnology and Oceanography*, 66, 3472–3488. <https://doi.org/10.1002/lno.11892>
- Sherman, K., & Duda, A. M. (1999). Large marine ecosystems: An emerging paradigm for fishery sustainability. *Fisheries*, 24, 15–26. [https://doi.org/10.1577/1548-8446\(1999\)024<0015:LME>2.0.CO;2](https://doi.org/10.1577/1548-8446(1999)024<0015:LME>2.0.CO;2)
- Silva, E. N. S., Gangopadhyay, A., Fay, G., Welandawe, M. K. V., Gawarkiewicz, G., Silver, A. M., Monim, M., & Clark, J. (2020). A survival analysis of the Gulf Stream warm core rings. *Journal of Geophysical Research, Oceans*, 125. <https://doi.org/10.1029/2020JC016507>
- Silver, A., Gangopadhyay, A., Gawarkiewicz, G., Andres, M., Flierl, G., & Clark, J. (2022). Spatial variability of movement, structure, and formation of warm core rings in the Northwest Atlantic Slope Sea. *Journal of Geophysical Research, Oceans* 127:e2022JC018737, 127. <https://doi.org/10.1029/2022JC018737>
- Silver, A., Gangopadhyay, A., Gawarkiewicz, G., Silva, E. N. S., & Clark, J. (2021). Interannual and seasonal asymmetries in Gulf Stream Ring Formations from 1980 to 2019. *Scientific Reports*, 11, 2207. <https://doi.org/10.1038/s41598-021-81827-y>
- Suberg, L. A., Miller, P. I., & Wynn, R. B. (2019). On the use of satellite-derived frontal metrics in time series analyses of shelf-sea fronts, a study of the Celtic Sea. *Deep Sea Research Part I: Oceanographic Research Papers*, 149, 103033. <https://doi.org/10.1016/j.dsr.2019.04.011>
- Tolimieri, N., Haltuch, M. A., Lee, Q., Jacox, M. G., & Bograd, S. J. (2018). Oceanographic drivers of sablefish recruitment in the California current. *Fisheries Oceanography*, 27, 458–474. <https://doi.org/10.1111/fog.12266>
- Townsend, D. W., Pettigrew, N. R., Thomas, M. A., Neary, M. G., McGillicuddy, D. J., & O'Donnell, J. (2015). Water masses and nutrient sources to the Gulf of Maine. *Journal of Marine Research*, 73, 93–122. <https://doi.org/10.1357/002224015815848811>
- Townsend, D. W., Thomas, A. C., Mayer, L. M., Thomas, M. A., & Quinlan, J. A. (2006). Oceanography of the Northwest Atlantic continental shelf (1, W). *The Sea: The Global Coastal Ocean: Interdisciplinary Regional Studies and Syntheses*, 14, 119–168.
- Turner, K. J., Mouw, C. B., Hyde, K. J. W., Morse, R., & Ciochetto, A. B. (2021). Optimization and assessment of phytoplankton size class algorithms for ocean color data on the Northeast U.S. continental shelf. *Remote Sensing of Environment*, 267, 112729. <https://doi.org/10.1016/j.rse.2021.112729>
- Wood, S. (2017). *Generalized additive models: an introduction with R* (2nd ed.). Chapman and Hall/CRC. <https://doi.org/10.1201/9781315370279>
- Wood, S. N. (2011). Fast stable restricted maximum likelihood and marginal likelihood estimation of semiparametric generalized linear models. *Journal of the Royal Statistical Society, Series B (Statistical Methodology)*, 73, 3–36. <https://doi.org/10.1111/j.1467-9868.2010.00749.x>
- Zhang, W. G., & Gawarkiewicz, G. G. (2015). Dynamics of the direct intrusion of Gulf Stream ring water onto the Mid-Atlantic Bight shelf. *Geophysical Research Letters*, 42(18), 7687–7695.

## SUPPORTING INFORMATION

Additional supporting information can be found online in the Supporting Information section at the end of this article.

**How to cite this article:** Salois, S. L., Hyde, K. J. W., Silver, A., Lowman, B. A., Gangopadhyay, A., Gawarkiewicz, G., Mercer, A. J. M., Manderson, J. P., Gaichas, S. K., Hocking, D. J., Galuardi, B., Jones, A. W., Kaelin, J., DiDomenico, G., Almeida, K., Bright, B., & Lapp, M. (2023). Shelf break exchange processes influence the availability of the northern shortfin squid, *Illex illecebrosus*, in the Northwest Atlantic. *Fisheries Oceanography*, 1–18. <https://doi.org/10.1111/fog.12640>